Article title: Climate Change impact on wave energy in the Persian Gulf

Journal name: Ocean Dynamics

Authors:
- Bahareh Kamranzad, PhD, Ocean Engineering and Technology Research Center, Iranian National Institute for Oceanography and Atmospheric Science, No. 3, Etemadzadeh St., Fatemi Ave., Tehran, 1411813389, IR Iran, Fax: +98-21-66944869
E-mail address: kamranzad@inio.ac.ir

- Amir Etemad-Shahidi*, PhD, Griffith School of Engineering, Gold Coast campus
Griffith University QLD 4222, Australia
Tel: +61-07-5552 9267, Fax: +61-07-5552-8065
* Corresponding Author, E-mail: a.etemadshahidi@griffith.edu.au

-Vahid Chegini, PhD, Ocean Engineering and Technology Research Center, Iranian National Institute for Oceanography and Atmospheric Science, No. 3, Etemadzadeh St., Fatemi Ave., Tehran, 1411813389, IR Iran, Fax: +98-21-66944869
E-mail address: vahid.chegini@gmail.com

- Abbas Yeganeh-Bakhtiary, PhD, School of Civil Engineering, Iran University of Science and Technology,
Tehran, Iran, P.O. Box 16765-163
E-mail address: yeganeh@iust.ac.ir

Abstract

Excessive usage of fossil fuels and high emission of greenhouse gases have increased the earth's temperature, and consequently have changed the patterns of natural phenomena such as wind speed, wave height, etc. Renewable energy resources are ideal alternatives to reduce the negative effects of increasing greenhouse gases emission and climate change. However, these energy sources are also sensitive to changing climate. In this study, the effect of climate change on wave energy in the Persian Gulf is investigated. For this purpose, future wind data obtained from CGCM3.1 model were downscaled using a hybrid approach and modification factors were computed based on local wind data (ECMWF) and applied to control and future CGCM3.1 wind data. Downscaled wind data was used to generate the wave characteristics in the future based on A2, B1 and A1B scenarios, while ECMWF wind field was used to generate the wave characteristics in the control period. The results of these two 30-yearly wave modelings using SWAN model showed that the average wave power changes slightly in the future. Assessment of wave power spatial distribution showed that the reduction of the average wave power is more in middle parts of the Persian Gulf. Investigation of wave power distribution in two coastal stations (Boushehr and Assalouyeh ports) indicated that the annual wave energy will decrease in both stations while the wave power distribution for different intervals of significant wave height and peak period will also change in Assalouyeh according to all scenarios.

Keywords: wave energy; climate change; CGCM3.1; Persian Gulf

1. Introduction

Global observations indicate that the worldwide temperature has increased by about 0.74ºC per century (Solomon et al., 2007). Satellite measurements show that the extent of snow cover has decreased about 10% since the late 1960s. International Panel on Climate Change (IPCC) also highlighted the changing precipitation in the middle and high latitudes of the Northern Hemisphere. In addition, the rate of global mean sea level rise is determined to be 1 to 2 mm/yr during the 20^{th} century (Ghosh and Misra, 2010). A rising trend of wave height is also reported in North East Atlantic since the late 1980s, which is estimated to be about 2% per year and around 30 to 50% in thirty years (Carter and Draper, 1988; Carter and Bacon, 1991). Furthermore, the recent investigations indicate that there is an increase in

mean sea level, significant wave height and average wind speed to about 30 cm/century, 7 to 10 cm/century and 1 m/s/century, respectively (Sündermann et al., 2001). Factors causing climate change include ocean processes such as the motion of tectonic plates, variations in solar radiation, variations in the earth's orbit, changes in greenhouse gas concentrations due to the human activities, etc. Since greenhouse gases greatly affect the temperature of the earth, increase in their emission cause increase in earth temperature. Recent studies also show that one of the main effective parameters in global warming is the increase of the greenhouse gases emission due to the development activities (Houghton et al., 2001). Indeed, a high level of carbon dioxide produced by excessive use of fossil fuels is the main reason of global warming (Houghton et al., 2001). Global warming due to the increasing greenhouse gases emission can affect highly on environment and human activities such as sea level rise, flooding in coastal areas, erosion of sandy beaches, etc. (Kont et al., 2003).

Renewable energy resources are alternatives for the fossil fuels. These sources of energy are green and clean and can reduce the negative effects of increasing in greenhouse gases emission and global warming. Marine renewable energies are valuable energy resources in areas adjacent to the seas or oceans (e.g. Morim et al., 2014). International Energy Agency (IEA) (IEA-OES, 2007) declared that the global oceans contain the capacity of 93100 TWh/yr, which is the same or greater than the current global power generation capacity (17400 TWh/yr) (Tsai et al., 2012). Among the marine renewable energy resources, waves contain the highest energy density (Leijon et al., 2003). Moreover, predictability as well as the low visual and environmental impact makes the wave energy a valuable renewable energy resource (Iglesias et al., 2009). However, the amount of energy captured from the renewable resources can be influenced by climate change (Breslow and Sailor, 2002; Harrison and Wallace, 2005). Therefore, it is essential to investigate the effects of climate change on renewable energy resources. Changes in the wind or wave patterns induced by the climate change can be evaluated based on the field observations or the climate prediction models. General Circulation Models or Global Climate Models (GCMs) are developed for simulation of global climate response due to increasing greenhouse gases emission with different emission scenarios in low resolutions while Regional Climate Models (RCMs) are developed as local models with higher resolution for considering the different responses of climate to the rising greenhouse gases' emission.

There are many studies around the world investigating the effect of climate change on wind or wave regime using different methods. For example, Chini et al. (2010), using data obtained from a

continental shelf climatic wave model, showed that the emission scenarios result in an increase of 12% for extreme wave height for 100-yr return period in eastern coasts of UK. According to studies of Harrison and Wallace (2005), wind speed has increased about 15 to 20% during four decades. Reeve et al. (2011) used both global and regional climate models for assessing the impact of climate change on wave energy in UK and showed that the wave energy will increase by about 2 to 3% according to A1B scenario and will decrease by about 1 to 3% according to B1 scenario. Pryor et al. (2004) investigated the temporal and spatial variation in wind speed and power using the data obtained from a GCM, i.e., HadCM3 (Stratton, 1999) and local wind fields, i.e., ECMWF (Simmons and Gibson, 2000) and NCEP/NCAR (Kalnay et al., 1996) in Baltic Sea and indicated that the wind power has no significant change in the future.

Charles et al. (2012) used the climate model ARPEGE-Climat (Gibelin and Déqué 2003) and showed that the wave height will decrease in the future about 20 cm in summer in the Bay of Biscay. Lionello et al. (2003), using downscaled ECHAM-4 model in the Adriatic Sea and found that the extreme wave height will decrease in the future. In Mediterranean, the results obtained from a regional climate model showed that the distribution of significant wave height will change seasonally (Lionello et al., 2008). Segal et al. (2001) used RegCM2 (Giorgi et al., 1993) model and represented that the daily average wind power will decrease up to 30% in US. Breslow and Sailor (2002) pointed out that the climate change causes a reduction of 10 to 15% in wind speed and therefore, 30 to 40% for wind power. Pereira de Lucena et al. (2010) used a regional climate model in Brazil and indicated that the wind power will not change in the future.

Considering the growth of population and industries around the seas adjacent to Iran, providing the electricity in future is a very important issue. The marine energies and especially the wave energy are appropriate candidates for achieving this purpose. Hence, recently, marine renewable energy resources such as wind and wave power potentials have been widely investigated in Iran for its adjacent seas, i.e., Persian Gulf, Gulf of Oman and Caspian Sea. Abbaspour and Rahimi (2011) evaluated the wave energy potential in some coastal locations in the northern coasts of the Persian Gulf. Assessment of wave energy distribution in the whole Persian Gulf was carried out by Etemad-Shahidi and Kamranzad (2011) and Kamranzad et al. (2013a) and the wave energy potential in selected areas was investigated by Kamranzad et al. (2014). Evaluation of wave energy potential in the northern coasts of the Gulf of Oman was also carried out by Saket and Etemad-Shahidi (2012). Similarly, Kamranzad et al. (2012),

Rusu and Onea (2013) and Hadadpour et al. (2014a, 2014b) estimated the wave energy potential in the Caspian Sea. Therefore, studying the climate change impact on the estimated renewable energy resources in Iran is of great importance to understand how the availability of these resources will change in the future.

In this study, the effect of climate change on wave energy is assessed in the Persian Gulf. For this purpose, data obtained from a Global Climate Model (GCM) are downscaled in the area using a hybrid downscaling method and the wind fields obtained from downscaled climate model and a local model are used for estimating and comparing the wave energy for two 30-yearly periods, i.e., the control period (1981 to 2010) and the future period (2071 to 2100). The comparison is carried out in both the whole domain and in selected coastal areas in terms of wave power distribution.

2. Study area and dataset

Persian Gulf is formed from the extension of the Indian Ocean. It is located in the south of Iran and is also adjacent to the countries in Arabian Peninsula. It is an important area due to the existence of rich resources of oil and gas, as well as transportations and fisheries (figure 1). However, these resources of fossil fuels will finish in the future. In addition, regarding their negative effects on climate, it is important to replace them with clean energy resources. There are many important locations in north of Persian Gulf where the assessment of renewable energies and especially wave energy is of great importance, such as Boushehr and Assalouyeh ports.

Dataset used in this study for wave modeling and wave power estimation consist of wind, wave and bathymetry data. Two wave modeling was carried out in control and future periods. For this purpose, the wind data obtained from European Centre for Medium-Range Weather Forecasts (ECMWF) wind field with 0.5º resolution in both longitude and latitude was used for the modeling purpose in the control period (figure 2). This wind field was evaluated and modified in the Persian Gulf to achieve the most consistency with the local measured winds (Mazaheri et al., 2013).

The third generation Coupled Global Climate Model (CGCM3.1) developed by the Canadian Center for Climate Modelling and Analysis (CCCMA) with T63 resolution (2.81º in longitudes and about 2.8º in latitudes) with A2, B1 and A1B emission scenarios were used for the wave modeling in the future. These three scenarios were selected since they represent the highest, lowest and the average CO_2 emissions, respectively (IPCC, 2000). This model gives the daily wind data in both control (1850 to

2000, named 20C3M) and future (2001 to 2100 using data obtained from A2, B1 and A1B scenarios) periods (figure 2). More information about this model can be found in Flato and Boer (2001) and Kim et al. (2002, 2003). This model was used in Persian Gulf and was compared to the local wind field (ECMWF) in control period, and its variation during the future period is investigated in the study area (Kamranzad et al., 2013b).

Bathymetry data with 1 minute (about 1.67 km) spatial resolution obtained from the NOAA's National Geophysical Data Center (NGDC) website was used as the model input and hourly measured wave data prodived by two buoys in the Persian Gulf was used for the model calibration and verification. One of the buoys was located near Boushehr at 50.5º E and 28.58º N in a depth of about 28 m; while the other one was located in Assalouyeh at 52.55º E and 27.51º N in a depth of about 50 m (figure 1). Moreover, the wave modeling was carried out using SWAN (Simulating WAves Nearshore) model (Booij et al., 1999) covering the whole domain.

3. Downscaling and Modeling

3.1. Downscaling method

As the resolution of CGCM3.1 is very low and covers limited points in Persian Gulf, data downscaling is required. Downscaling is a process in which the global data is transformed into higher resolution data to achieve the most possible consistency with the local data. There are two main approaches for downscaling; statistical and dynamical downscaling (Fowler et al., 2007). In dynamical downscaling a Regional Climate Model (RCM) is nested in a Global Climate Model (GCM) and supplies the boundary condition from the GCM data. Statistical downscaling is the procedure of obtaining a relationship between the predictors (variables obtained from GCMs) and predictands (local variables) (e.g. Sailor et al., 2000) and applying the relationship to the future data assuming that the said relationship remains the same in the future as it is in the control period.

In this study, a hybrid downscaling approach, i.e., a combination of dynamical and statistical downscaling methods was utilized. In this method, a fine grid was considered based on ECMWF grid and resolution (0.5º). This wind field supplies the time series of the wind characteristics from CGCM3.1 data in the corresponding grid points to CGCM3.1 as the boundary conditions and computes the wind data in other grid points using Inverse-Distance Weighting (IDW) method (Burrough and McDonnell, 1998). Then, comparing to ECMWF data in each corresponding grid point, the data is

modified using a statistical downscaling. Assuming that the modification factors in the future were similar to those of the control period, they were applied on the interpolated CGCM3.1 wind in the future (for each scenario, separately) and the resulting downscaled wind fields are used for wave modeling in the future. Control period was considered from 1981 to 2010 in which, both ECMWF and CGCM3.1 were available. CGCM3.1 data in control period consists of 20C3M data (from 1981 to 2000) and A2, B1 and A1B scenarios data (from 2001 to 2010).

Comparison of CGCM3.1 and ECMWF wind fields was carried out in the corresponding grid points by Kamranzad et al. (2013b) and the results showed that the existing differences between these two winds are in terms of both wind speed and direction. Therefore, different modification factors were considered for each wind component, separately in order to modify both wind speed and wind direction, simultaneously. Since the above-mentioned study illustrated that the difference between ECMWF and CGCM3.1 varies spatially, the modification factor should vary for each grid point. Since the objective of this study was to find the variations of average wave energy, the modification factor was determined to modify the average wind speed based on the Bias minimization between CGCM3.1 and ECMWF wind components. Hence, the monthly average of absolute values of each wind component (u as the wind speed in x-direction and v as the wind speed in y-direction) for two wind sources i.e., ECMWF and CGCM3.1 were compared and the monthly modification factors were determined as constant factors in each grid point, for each wind component, for each scenario.

This is similar to the method that Breslow and Sailor (2002) used for downscaling a GCM to estimate the change in wind power in US. However, they calculated a modification factor for the wind speed parameter (instead of wind components) in each gird point for the total control period (instead of monthly factors). The modification factors for the monthly average of absolute wind components were determined by:

$$\beta_u = \frac{|u|_{ECMWF(monthly\ average)}}{|u|_{CGCM3.1(monthly\ average)}} \quad (1)$$

$$\beta_v = \frac{|v|_{ECMWF(monthly\ average)}}{|v|_{CGCM3.1(monthly\ average)}} \quad (2)$$

in which, β_u and β_v represent the modification factors for u and v components of the wind speed, respectively.

β factors were obtained for 30-yearly data in the control period (1981 to 2010) for each month separately; consisting of the combination of both 20C3M data (1981-2010) and scenario data (2001-2010). Hence, three combinations of 20C3M with three scenarios were obtained which led to three series of modification factors (for each scenario) (figure 2). In order to save space, only modification factors for months June to August are shown in figures 3 to 5, respectively and the modification factors for other months are shown in appendix (figures 15 to 23). The results show that β_v was larger than β_u in the northwest parts of the Persian Gulf. It means that the *v*-component of the CGCM3.1 wind is underestimated more than the *u*-component. It must be mentioned that the prevailing wind regime in the Persian Gulf, particularly in northwest parts, is the so-called Shamal wind; blowing from the northwest in summer (Thoppil and Hogan, 2010). Therefore, CGCM3.1 dominant wind directions should be slightly modified to W-NW direction (see also Kamranzad et al. 2013b). In addition, the differences between β_u and β_v increases in months June, July and August when the Shamal wind is dominant.

Unlike the northwest parts of Persian Gulf, β_u is larger than β_v in Strait of Hormuz which means the horizontal component is underestimated compared to vertical one. Summary of β figures illustrate that monthly modification factors are relatively similar for different scenarios, except for some months in which both β_u and β_v are higher for B1 scenario. This means that there is a larger difference between B1 scenario and ECMWF data rather than A1B and A2 scenarios. These spatially varied β factors were also applied to the interpolated CGCM3.1 wind field in the future period (2071 to 2100) for each component for each month, separately. For this purpose, each month's data was extracted during 30-yearly period and the modification factors for each grid point were applied to two components of the wind speed, separately. This was done for three different scenarios, separately. Then, the modified time series of each grid point were sorted by date to achieve the time series of modified wind data in all grid points during the 30-year period. The resulting wind field was finally used for wave modeling in the future period.

3.2. Wave modeling and wave power estimation

Numerical wave modeling was carried out using SWAN numerical model version 40.72. SWAN is a spectral model developed for estimation of the wave characteristics in nearshore areas. It can solve the transport equation (WAMDI group, 1988; Komen et al., 1994) without considering any limitation on

the wave energy spectral form (Bolaños-Sanchez et al., 2007). SWAN also considers the effective processes for small scale, high resolution applications (generation, dissipation and nonlinear wave-wave interactions) (Ris et al., 1999).

The action balance equation is the basic equation used in the SWAN and for the Cartesian coordinates is defined as (Ris et al., 1999):

$$\frac{\partial}{\partial t}N+\frac{\partial}{\partial x}c_x N+\frac{\partial}{\partial y}c_y N+\frac{\partial}{\partial \sigma}c_\sigma N+\frac{\partial}{\partial \theta}c_\theta N=\frac{S}{\sigma} \quad (3)$$

in which N represents the action density and is a function of intrinsic frequency (σ), wave direction (θ), horizontal coordinates (x and y) and the time (t). The first term on the left-hand side indicates the temporal change of N and the next two terms illustrate the propagation of N in geographical x and y space, respectively (in which, c_x and c_y are the propagation velocities in x and y directions, respectively). The fourth term demonstrates the shifting effect of the relative frequency due to variations in depth and currents (in which, c_σ shows the propagation velocity in σ space). The last term on the left-hand side of the equation represents the depth and current-induced refraction (in which, c_θ shows the propagation velocity in θ space). The term S on the right-hand side of the equation is a function of σ, θ, x, y and t. S consists of effects of the generation by wind, dissipation (by white-capping, depth induced wave breaking and bottom friction) and nonlinear wave-wave interactions (Ris et al., 1999).

In order to produce the wave climate in the future, one model was used in control period to estimate the wave energy based on local wind data and three models were used to be calibrated in the control period using downscaled wind fields obtained from three scenarios,. Therefore, four models were considered with different tuning parameters. To obtain the time series of the wave characteristics, these four models were executed in two dimensional nonstationary mode. It was noted by Moeini and Etemad-Shahidi (2007) and Moeini et al. (2010, 2014) that using the theory of Komen et al. (1984) wind input parameterization yields more accurate results for the prediction of significant wave height. Therefore, this option was used in four models. Computational grid for all models was specified from 48° E to 57° E and 23° N to 31° N (figure1) with the spatial resolution of 0.1° and temporal resolution of 20 min. Output data were obtained in a grid with 0.2° spatial resolution in all models.

Wave power is calculated using the time series of significant wave height and peak period obtained from the numerical wave modeling. This method is one of the most common methods for calculating

the wave power over long periods (e.g. Henfridsson et al., 2007). According to the following equation, the wave energy density is obtained by (Hughes and Heap, 2010):

$$E = \frac{1}{16}\rho g {H_s}^2 \quad (4)$$

in which ρ is the water density, g is the gravitational acceleration and H_s is the significant wave height and the wave power is defined as:

$$P = EC_g = ECn \quad (5)$$

where C is the wave speed and n is the ratio between the wave group speed and wave speed. C is equal to wave length divided by the wave period (T) and is equal to $gT/2\pi$ in deep water. The approximate value of n is equal to 0.5 in deep water. Thus, the wave power is calculated as follow (Abbaspour and Rahimi, 2011).

$$P = \frac{1}{16}\rho g H_s^2 \times \frac{gT}{2\pi} \times 0.5 \approx 0.49 H_s^2 T \quad (6)$$

Since the real sea states include a large number of regular waves, the mixture of different amplitudes, frequencies and directions is described using a variance spectral density function. The wave power per unit width of the irregular waves in deep water can be obtained by:

$$P \approx 0.49 H_s^2 T_e \quad (7)$$

in which T_e is the energy period. When peak period (T_p) is available, T_e is equal to T_p multiplied by a factor that is equal to 0.9 if the standard JONSWAP spectrum with a peak enhancement factor of γ=0.33 is assumed (Abbaspour and Rahimi, 2011).

Wave modeling consisted of four simulations for two different periods, i.e., one for control (1981 to 2010) and three (A2, B1 and A1B) for future (2071 to 2100). Wave modeling in the control period was carried out before to estimate the wave energy distribution in the Persian Gulf by Kamranzad et al. (2013a and 2014). Wave modeling for the future period (2071 to 2100) was conducted using downscaled wind fields obtained from A2, B1 and A1B scenarios data according to section 3.1.

Due to the lack of future wave data, the model was first calibrated and verified in the control period using three downscaled wind fields for three scenarios. The three calibrated and verified wave models in the control period were employed to generate three 30-years wave fields in the future, for each scenario (separately); without changing any tuning parameters. The input wind field was the only parameter that was changed in the future wave modeling compared to control wave modeling

calibration. Both modelings were carried out using the downscaled CGCM3.1 wind field for three scenarios, i.e., A2, B1 and A1B.

The calibration and verification of the model were conducted during a 5-year period (from 2004 to 2008) and the results of wave modeling using the hybrid downscaled CGCM3.1 were compared to results of wave modeling using local wind (ECMWF) that was previously calibrated (Kamranzad et al., 2013a).

Using downscaled wind data obtained from A2, B1 and A1B scenarios, three wave models were calibrated based on bias minimization of the wave power parameter in eight stations (table 1). The whitecapping dissipation coefficient as the tuning parameter (Kamranzad et al., 2013a) varies in each model because of the different wind conditions for four models (using three scenarios for the future) and is shown in table 2. For quantitative comparison of the results, *Bias* and Mean Square Error (*MSE*) were calculated using the following equations.

$$Bias = \bar{y} - \bar{x} \tag{8}$$

$$MSE = \frac{\sum_i (x_i - y_i)^2}{n} \tag{9}$$

here x and y are the measured and modeled values, respectively, $\bar{x}$ and $\bar{y}$ are their average and n shows the number of data. Table 3 presents the accuracy metrics in each point for both calibration and verification done for each scenario. The calibrated and verified model was then executed for the future period (2071 to 2100) using three scenarios of downscaled data. The results of wave modeling in two 30-yearly control and future periods were finally used to determine the time series of wave power in the domain.

4. Results and discussion

Wave power distributions in the Persian Gulf using data obtained from the wave modeling in control and future periods (A2, B1 and A1B scenarios) are depicted in figure 6. As seen from the figure, there is no significant change in annual average wave power in the future, comparing to the control period. In addition, the change in annual average wave power using downscaled wind field obtained from A2 and B1 scenarios show the largest and smallest changes compared to the control period, respectively.

For further assessment, three stations were selected in the western, middle and eastern parts of the Persian Gulf named W, M and E, respectively (figure 1). Time series of the wave powers were extracted in these stations from all four wave models (in control and future periods) and the annual average wave powers were obtained (figure 7). Figure 7 shows that the annual wave power decreases during years 1990 to 2000 in the control period. Wave power characteristics of the stations W, M and E in the control period have been investigated before by Kamranzad et al. (2013a) and it was pointed out that there was a slight reduction in annual average wind speed for the years 1990 to 2000, causing a reduction in total average of the wave powers. For example, a reduction of about 24% in annual average wind speed for the period of 1990 to 2000 led to a 90% reduction in annual average wave power at station M (Kamranzad et al., 2013a). However, the 30-yearly average wave power has no significant difference in the future comparing to the control period (figure 6). According to figure 7, the future annual average wave powers were higher than annual average wave powers in 1990 to 2000 and were less in other periods and no decadal variations was observed in the 30-yearly future period.

At station W, the average of wave power in the control period is about 1.23 KW/m while it is 1.20, 1.21 and 1.27 KW/m considering A1B, A2 and B1 scenarios, respectively. Therefore, the wave power in the future will decrease about 2% for A1B and A2 scenarios and increase about 3 % for B1 scenario. At station M, the average wave power in the control period is 2.13 KW/m and the future average wave power is 1.52, 1.37 and 1.66 KW/m considering A1B, A2 and B1 scenarios, respectively, that means a reduction of about 29%, 36% and 22% in the future average wave power for A1B, A2 and B1 scenarios, respectively. The average wave power in the control period is about 0.52 KW/m at station E while it reduces to 0.46, 0.39 and 0.47 KW/m for A1B, A2 and B1 scenarios, respectively in the future. This reduction is about 12%, 25% and 10% for A1B, A2 and B1 scenarios, respectively. It can be concluded that the wave power reduction is large in the station M, located in the middle parts of the Persian Gulf. In addition, the least amount of future wave power is obtained based on the data obtained from A2 scenario.

Wave power roses are plotted for the control and future periods for stations W, M and E in figures 8 to 10. Figure 8 shows that the dominant wave direction in station W changes from NW in the control period to W-NW in the future according to A1B and A2 scenarios while B1 scenario indicates the same direction as the control period. In station M, the dominant wave direction is NW in the control period,

while it is shown W-NW by all scenarios in the future (figure 9). According to figure 10, the dominant wave direction in station E is SW and no change in the future is illustrated.

One of the important characteristics of the wave power for selecting the most appropriate wave energy converter is its distribution in different intervals of the wave height and peak period to achieve the highest efficiency. For this purpose, two coastal sites were selected in the Persian Gulf, based on the wave power spatial distribution and the importance of the locations. These two selected sites are Boushehr and Assalouyeh ports. The most proper location for installation of a wave energy converter was selected based on criteria such as wave power, depth and distance from the coast. More information about the details of wave power assessment in these coastal locations can be found in Kamranzad et al. (2014). The wave power distribution based on the different significant wave heights and peak periods in Boushehr and Assalouyeh ports for the control and future periods (for A2, B1 and A1B scenarios) are plotted in figures 11 to 14.

Comparison of figures 11 to 14 illustrates that in Boushehr, the highest wave energy can be obtained from significant wave heights of 1 to 1.25 m and peak periods of 5.5 to 6 s for both control and future scenarios. The maximum wave energy in the future is about 0.42, 0.41 and 0.47 MWh/m for A1B, A2 and B1 scenarios, respectively while it is 0.65 MWh/m for the control period, i.e., the maximum wave energy will decrease about 33% in the future.

According to figure 11, the highest annual wave energy in Assalouyeh is available for the significant wave heights of 1.5 to 2 m and peak periods of 5.5 to 6 s for the control period and the resulting wave power for this range is about 7 KW/m. The highest future annual wave energy in the future can be captured from the significant wave heights of 1 to 1.25 m and peak periods of 5.5 to 6 s for all scenarios (figures 12 to 14). Moreover, the corresponding wave power is about 4 to 5 KW/m which is less than that of the control period. In addition, the maximum annual wave energy decreased in the future, according to all scenarios. It is about 0.34, 0.33 and 0.35 MWh/m for A1B, A2 and B1 scenarios showing a reduction when compared to the energy in the control period (1.15 MWh/m).It can be concluded that although the wave power decreases for the future scenarios near Boushehr port, its distribution has a slight change in the future. However, this issue is to some extent different in Assalouyeh port. Where in Assalouyeh both the wave power values and its distribution will change in the future in all considered scenarios. This will considerably affect the type of wave energy converter that will be used for in these areas.

5. Summary and Conclusion

The wave energy potential as a renewable energy resource has assessed before in Persian Gulf based on the data obtained from the past and current period. In order to estimate the future wave power, assessment of the effect of climate change on wave power characteristics is very important. Therefore, in this study, the impact of climate change on wave energy was investigated in the Persian Gulf. To achieve this purpose, four wave modeling consisting of one in control and three scenarios in future were carried out in 30-yearly periods (1981 to 2000 and 2071 to 2100, respectively). Wave modeling in the control period was carried out using a high resolution local wind field (ECMWF) while the wave modeling for the future period was conducted using a downscaled wind field obtained from CGCM3.1 model considering A2, B1 and A1B scenarios.

CGCM3.1 was downscaled in the Persian Gulf using a hybrid approach in which the modification factors were calculated monthly for each wind component in different scenarios, separately. Comparison of the estimated wave power in control and future periods indicated that A2 and B1 scenarios showed the largest and smallest changes in the average wave power, respectively. However, no significant change in annual average wave power in the future was observed compared to the control period.

Assessment of temporal variation of the wave power in three stations (W, M and E) illustrated that the wave power reduces in years between 1990 to 2000 in the control period and the future wave powers are higher than the wave powers in this 10-yearly period and they are lower than the wave power in the remaining years of the control period. Therefore, totally estimated, the average 30-yeraly wave power in future has no significant change comparing to the average 30-yeraly wave power in control period.

The results showed that the wave power marginally decreases in the future in station W (about 2%) according to A1B and A2 scenarios and increases about 3% according to B1 scenario. At station M, reductions of about 29%, 36% and 22% are expected for average wave power according to A1B, A2 and B1 scenarios, respectively. The reduction in the future average wave power in station E are about 12%, 25% and 10% according to A1B, A2 and B1 scenarios, receptively.

Changes in the wave power distribution for different intervals of wave characteristics were also investigated in two other selected coastal stations, i.e., Boushehr and Assalouyeh ports. The results revealed that although the wave power will decrease in the future scenarios, their distribution will

remain nearly constant in the future in Boushehr port. However, both the wave power and its distribution in Assalouyeh will change in future. The maximum wave energy in Boushehr decreases from 0.6 MWh/m in the control period to 0.42, 0.41 and 0.47 MWh/m in the future according to A1B, A2 and B1 scenarios, respectively. The maximum annual wave energy in Assalouyeh will decrease in the future, according to all scenarios. It is about 0.34, 0.33 and 0.35 MWh/m for A1B, A2 and B1 scenarios showing a reduction when compared to its value in the control period (1.15 MWh/m).

Assessment of wave power distribution in two coastal stations indicated that the annual wave energy will decrease in both stations while the wave power distribution for different intervals of significant wave height and peak period will only change in Assalouyeh considering all scenarios. However, the results showed that there is a negligible variation in the future annual average wave power. Because of changing of the maximum annual wave energy and the related intervals of significant wave height and peak period in the future, the impact of climate change should be considered in utilizing the wave energy resources and selection of wave energy converters.

Acknowledgement

We are thankful to SWAN group for providing the model and to the anonymous reviewers for their fruitful comments.

References

Abbaspour M, Rahimi R (2011) Iran atlas of offshore renewable energies. Renew Energy 36: 388-398

Bolaños-Sanchez R, Sanchez-Arcilla A, Cateura J (2007) Evaluation of two atmospheric models for wind–wave modelling in the NW Mediterranean. J Mar Syst 65:336-353

Booij N, Ris RC, Holthuijsen LH (1999) A third-generation wave model for coastal regions. 1. Model Description and validation. J Geophys Res 104:7649-7666

Breslow PB, Sailor DJ (2002) Vulnerability of wind power resources to climate change in the continental United States. Renew Energy 27:585-598

Burrough PA, McDonnell RA (1998) Principles of Geographical Information Systems. Oxford University Press, Oxford

Carter DJT., Bacon S (1991) Wave climate changes in the North Atlantic and North Sea. Intl J Climatology 11:545-558

Carter DJT, Draper L (1988) Has the north-east Atlantic become rougher? Nature 332-494

Charles E, Idier D, Delecluse P, Deque M, Le Cozannet G (2012) Climate change impact on waves in the Bay of Biscay, France. Ocean Dynamics 62:831-848

Chini N, Stansby P, Leake J, Wolf J, Roberts-Jones J, Lowe J (2010) The impact of sea level rise and climate change on inshore wave climate: A case study for East Anglia (UK). Coast Eng 57:973-984

Etemad-Shahidi A, Kamranzad B, Chegini V (2011) Wave energy estimation in the Persian Gulf. Proceedings of the International Conference on Environmental Pollution and Remediation, Ottawa, Ontario, Canada, pp. 223

Flato GM, Boer GJ (2001) Warming Asymmetry in Climate Change Simulations. Geophys Res Letters 28:195-198

Fowler HJ, Blenkinsop S, Tebaldi C (2007) Linking climate change modelling to impacts studies: recent advances in downscaling techniques for hydrological modelling. Intl J climatology 27:1547-1578

Ghosh S, Misra C (2010) Assessing Hydrological Impacts of Climate Change: Modeling Techniques and Challenges. The Open Hydrology J 4:115-121

Gibelin AL, Déqué M (2003) Anthropogenic climate change over the Mediterranean region simulated by a global variable resolution model. Climat Dynamics 20:327–339

Giorgi F, Marinucci MR, Bates GT, De Canio G (1993) Development of a second-generation regional climate model (RegCM2), I, boundary-layer and radiative transfer. Month Weather Rev 121:2794-2813

Hadadpour S, Etemad-Shahidi A, Kamranzad B (2014a) Wave energy forecasting using artificial neural networks in the Caspian Sea. Proc of the ICE-Maritime Eng, 167: 42-52

Hadadpour S, Etemad-Shahidi A, Jabbari E, Kamranzad B (2014b) Wave energy and hot spots in Anzali port. Energy, 74: 529-536.

Harrison GP, Wallace AR (2005) Sensitivity of Wave Energy to Climate Change. IEEE transactions on energy conversion 20:870-877

Henfridsson U, Neimane V, Strand K, Kapper R, Bernhoff H, Danielsson O, Leijon B, Sundberg J, Thorburn K, Ericsson E, Bergman K (2007) Wave energy potential in the Baltic Sea and the Danish part of the North Sea, with reflections on the Skagerrak. Renew Energy 32:2069-2084

Houghton JT, Ding Y, Griggs DJ, Noguer M, Van der Linden PJ (2001) The scientific basis, condition of working group I to the third assessment report of the intergovernmental panel on climate change. Cambridge, Cambridge University Press, UK

Hughes MG, Heap AD (2010) National-scale wave energy resource assessment for Australia. Renew Energy 35:1783-1791

Iglesias G, Lo´pez M, Carballo R, Castro A, Fraguela JA, Frigaard P (2009) Wave energy potential in Galicia (NW Spain). Renew Energy 34:2323–2333

Implementing agreement on ocean energy systems (IEA-OES) (2007) Annual report of international energy agency.

IPCC (2000) IPCC special report, emission scenarios. A Special Report of IPCC Working Group III.

Kalnay E, Kanamitsu M, Kistler R, Collins W, Deaven D, Gandin L, Iredell M, Saha S, White G, Woollen J, Zhu Y, Leetmaa A, Reynolds R (1996) The NCEP/NCAR 40 reanalysis project. Bulletin of the American Meteorological Society **77**:437-471

Kamranzad B, Etemad-Shahidi A, Chegini V (2012) Wave energy assessment in the Caspian Sea. 18th congress of the IAHR-APD, Jeju, South Korea, pp. 424-425

Kamranzad B, Etemad-Shahidi A, Chegini V (2013a) Assessment of wave energy variation in the Persian Gulf. Ocean Eng 70:72-80

Kamranzad B, Etemad-Shahidi A, Chegini V (2014) Wave energy potential in two specific sites in the northern Persian Gulf. Ocean Eng. Unpublished results.

Kamranzad B, Etemad-Shahidi A, Chegini V, Hadadpour S (2013b) Assessment of CGCM3.1 wind field in the Persian Gulf. J Coast Res 65:249-253

Kim SJ, Flato GM, Boer GJ (2003) A coupled climate model simulation of the Last Glacial Maximum, Part 2: approach to equilibrium. Climat Dynamics 20:635-661

Kim SJ, Flato GM, Boer GJ, McFarlane NA (2002) A coupled climate model simulation of the Last Glacial Maximum, Part 1: transient multi-decadal response. Climat Dynamics 19:515-537

Komen GJ, Cavaleri L, Donelan M, Hasselmann K, Hasselmann S, Janssen PAEM (1994) Dynamics and modeling of ocean waves. Cambridge University Press

Komen GJ, Hasselmann S, Hasselmann K (1984) On the existence of a fully developed wind sea spectrum. J Phys Oceanography 14:1271-1285

Kont A, Jaagus J, Aunap R (2003) Climate change scenarios and the effect of sea-level rise for Estonia. Global and Planetary Change 36:1-15

Leijon M, Bernhoff H, Berg M, Ågren O (2003) Economical considerations of renewable electric energy production-especially development of wave energy. Renew Energy 8:1201–1209

Lionello P, Cogo S, Galati MB, Sanna A (2008) The Mediterranean surface wave climate inferred from future scenario simulations. Global and Planetary Change 63:152-162

Lionello P, Nizzero A, Elvini E (2003) A procedure for estimating wind waves and storm-surge climate scenarios in a regional basin: the Adriatic Sea case. Climat Res 23:217–231

Mazaheri S, Kamranzad B, Hajivalie F (2013) Modification of 32 years ECMWF wind field using QuikSCAT data for wave hindcasting in Iranian Seas. J Coast Res SI 65:344-349

Moeini MH, Etemad-Shahidi A, (2007) Application of two numerical models for wave hindcasting in Lake Erie. Appl Ocean Res 29:137-145

Moeini MH, Etemad-Shahidi A, Chegini V (2010) Wave modeling and extreme value analysis off the northern coast of the Persian Gulf. Appl Ocean Res 32:209-218

Moeini, M.H., Etemad-Shahidi, A., Chegini, V. and Rahmani, I. (2012) Wave data assimilation using a hybrid approach in the Persian Gulf, Ocean Dyn, 62: 785-797

Moeini, M.H., Etemad-Shahidi, A., Chegini, V., Rahmani, I. Moghaddam, M. (2014) Error distribution and correction of the predicted wave characteristics over the Persian Gulf, Ocean Eng, 75: 81-89

Morim, J., Cartwright, N., Etemad-Shahidi, A., Strauss, D. and Hemmer, M. (2014) A review of wave energy estimates for nearshore shelf waters off Australia, Int J of Mar Energy, 7: 57-70

Pereira de Lucena AF, Szklo AS, Schaeffer R, Dutra RM (2010) The vulnerability of wind power to climate change in Brazil. Renew Energy 35:904-912

Pryor SC, Barthelmie RJ, Schoof JT (2004) Historical and prognostic changes in a normal wind year: A case study from the Baltic, Special topic conference: The science of making torque from wind. Delft (NL) 336-345

Reeve DE, Chen Y, Pan S, Magar V, Simmonds DJ, Zacharioudaki A (2011) An investigation of the impacts of climate change on wave energy generation: The Wave Hub, Cornwall, UK. Renew Energy 36:2404-2413

Ris RC, Holthuijsen LH, Booij N (1999) A third-generation wave model for coastal regions 2. Verification. J Geophys Res 104:7667-7681

Rusu E, Onea F (2013) Evaluation of the wind and wave energy along the Caspian Sea. Energy 50:1-14

Sailor DJ, Hu T, Li X, Rosen JN (2000) A neural network approach to local downscaling of GCM output for assessing wind power implications of climate change. Renew Energy19:359-378

Saket A, Etemad-Shahidi, A (2012) Wave energy potential along the northern coasts of the Gulf of Oman. Renew Energy 40:90-97

Segal M, Pan Z, Arritt RW, Takle ES (2001) On the potential change in wind power over the US due to increases of atmospheric greenhouse gases. Renew Energy 24:235-243

Simmons AJ, Gibson JK (2000) The ERA- 40 Project Plan. Available from http://www.ecmwf.int/: UK Meteorological Office, UK. p. 63

Solomon SD, Qin M, Manning M, Chen Z, Marquis M, Averyt KB, Tignor M, Miller HL (2007) The physical science basis, Contribution of Working Group I to the Fourth Assessment Report of the Intergovernmental Panel on Climate Change. Cambridge, Cambridge University Press, UK

Stratton RA (1999) A high resolution AMIP integration using the Hadley center model HadAM2b. Climat Dynamics 15:9-28

Sündermann J, Beddig S, Huthnance J, Mooers CNK (2001) Impact of climate change on the coastal zone: discussion and conclusions. Climat Res 18:1-3

Thoppil PG, Hogan PJ (2010) Persian Gulf response to a wintertime Shamal wind event. J Deep-Sea Res I 57:946-955

Tsai CP, Hwang CH, Hwa C, Cheng HY (2012) Study on the wave climate variation to the renewable wave energy assessment. Renew Energy 38:50-61

WAMDI group (1988) The WAM model-a third generation ocean wave prediction model. J Phys Oceanography 18:1775-1810

Figure Captions

Fig. 1 Study area, buoy location and stations W, M and E (after Kamranzad et al., 2013a)

Fig. 2 Detail of available data (ECMWF and CGCM3.1) and periods of hybrid downscaling and wave modeling

Fig. 3 β_u (left) and β_v (right) for A1B, A2 and B1 scenarios in June

Fig. 4 β_u (left) and β_v (right) for A1B, A2 and B1 scenarios in July

Fig. 5 β_u (left) and β_v (right) for A1B, A2 and B1 scenarios in August

Fig. 6 Annual average of wave power (KW/m) in Persian Gulf for control period (CTR) and scenarios

Fig. 7 Annual wave power (KW/m) in 30-yearly control and future periods in stations W, M and E

Fig. 8 Power roses in control and future periods in station W

Fig. 9 Power roses in control and future periods in station M

Fig. 10 Power roses in control and future periods in station E

Fig. 11 Wave power distribution in control period in (a) Boushehr and (b) Assalouyeh

Fig. 12 Wave power distribution in (a) Boushehr and (b) Assalouyeh according to A1B scenario

Fig. 13 Wave power distribution in (a) Boushehr and (b) Assalouyeh according to A2 scenario

Fig. 14 Wave power distribution in (a) Boushehr and (b) Assalouyeh according to B1 scenario

Table 1. Location of considered stations for calibration and verification

Station ID	Longitude	Latitude
C1	50.5	28.5
C2	52	26.5
C3	52.5	27.3
C4	55	26
C5	49.5	29
C6	51	27.5
C7	53	26
C8	56	26.5

Table 2. Values of tuning parameters for all models

Wind field	Whitecapping dissipation coefficient
A1B	6.40E-06
A2	6.50E-06
B1	6.65E-06

Table 3. Error indices for wave modeling using downscaled CGCM3.1

A1B				
Location	*Bias*		*MSE*	
	Calibration	Verification	Calibration	Verification
C1	0.14	0.02	0.57	0.48
C2	0.03	-0.04	0.61	0.73
C3	0.02	-0.02	0.30	0.35
C4	0.03	-0.01	0.48	0.56
C5	0.14	0.04	0.53	0.38
C6	0.07	-0.03	0.57	0.57
C7	0.08	0.06	0.59	0.76
C8	-0.07	-0.09	0.34	0.43
A2				
Location	*Bias*		*MSE*	
	Calibration	Verification	Calibration	Verification
C1	0.07	0.07	0.48	0.56
C2	0.01	-0.01	0.59	0.72
C3	0.01	0.00	0.31	0.37
C4	0.03	-0.02	0.48	0.50
C5	0.06	0.10	0.40	0.50
C6	0.02	0.01	0.51	0.61
C7	0.08	0.05	0.59	0.70
C8	-0.07	-0.10	0.35	0.39
B1				
Location	*Bias*		*MSE*	
	Calibration	Verification	Calibration	Verification
C1	0.10	0.05	0.52	0.48
C2	0.01	-0.06	0.67	0.61
C3	0.00	-0.03	0.33	0.31
C4	0.04	-0.02	0.59	0.52
C5	0.06	0.07	0.41	0.40
C6	0.02	-0.03	0.54	0.52
C7	0.08	0.04	0.74	0.64
C8	-0.07	-0.08	0.37	0.41

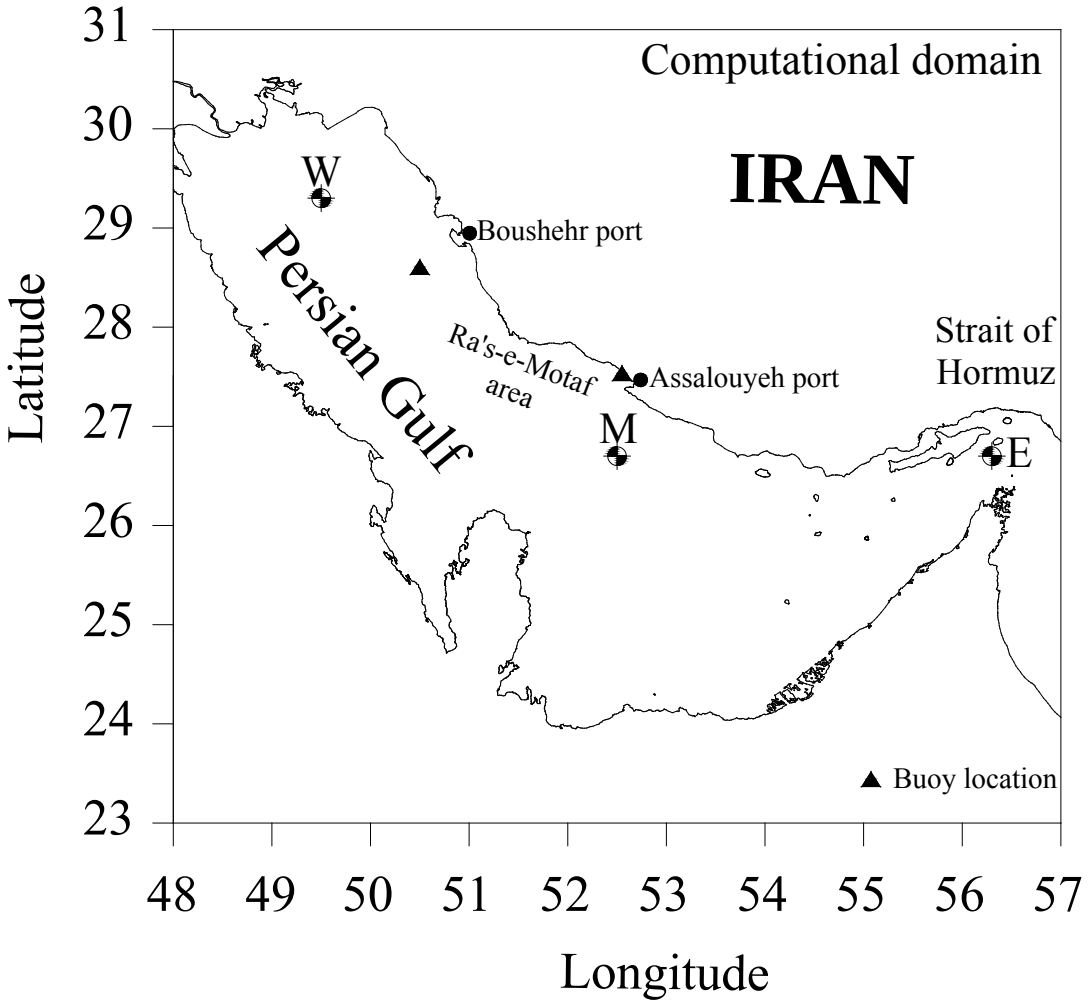

Fig. 1 Study area, buoy location and stations W, M and E (after Kamranzad et al., 2013a)

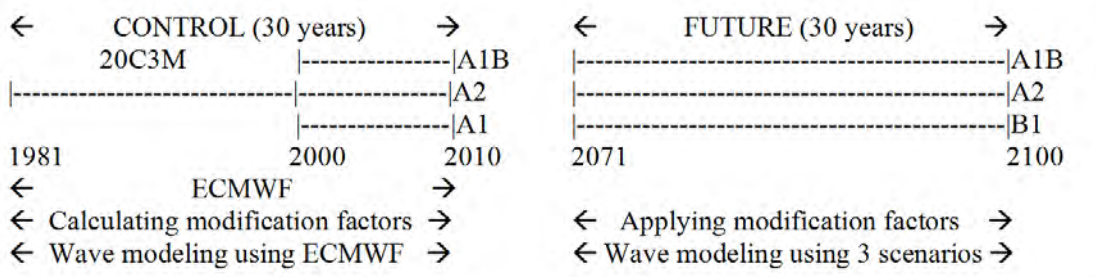

Fig. 2 Detail of available data (ECMWF and CGCM3.1) and periods of hybrid downscaling and wave modeling

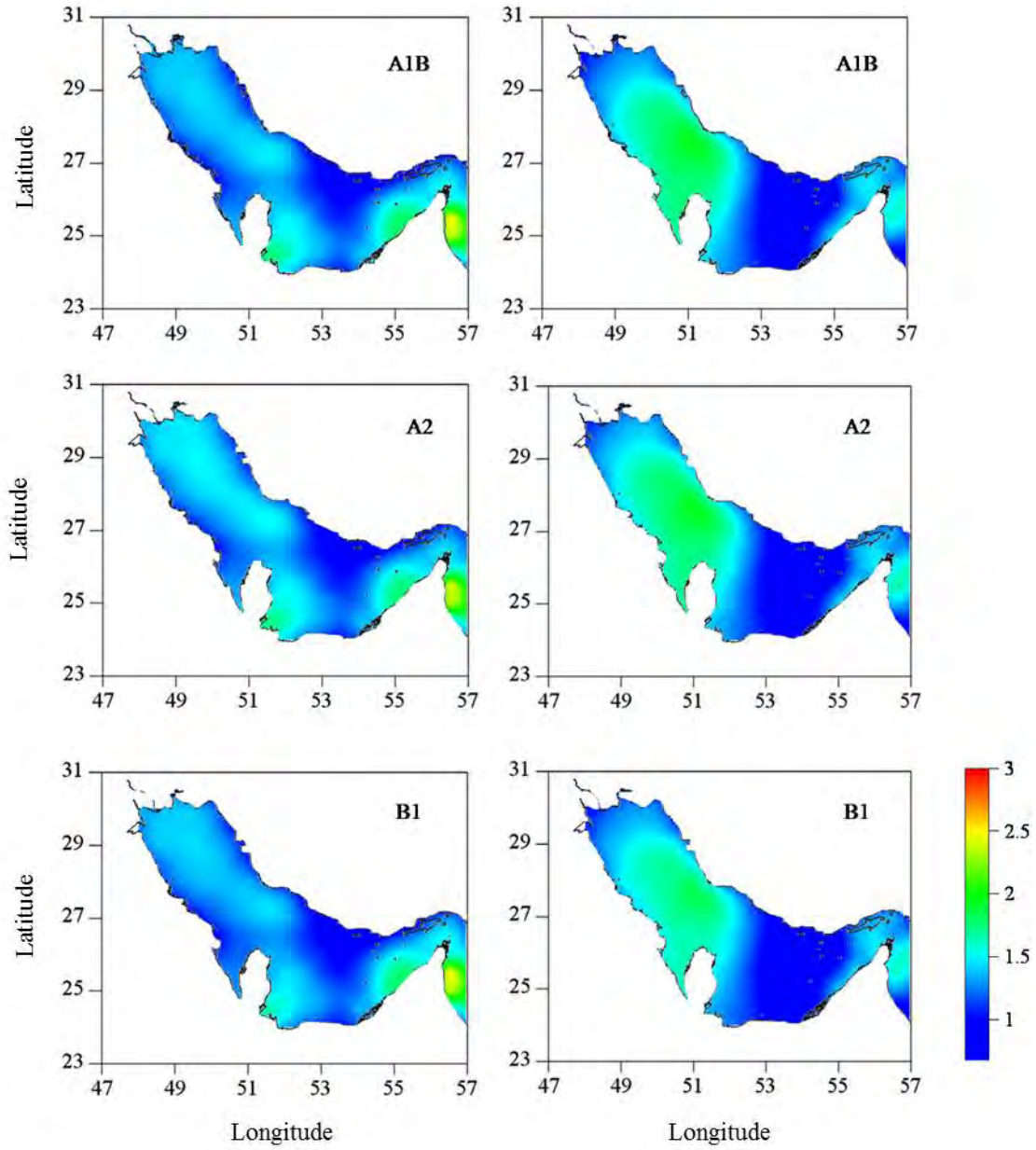

Fig. 3 β_u (left) and β_v (right) for A1B, A2 and B1 scenarios in June

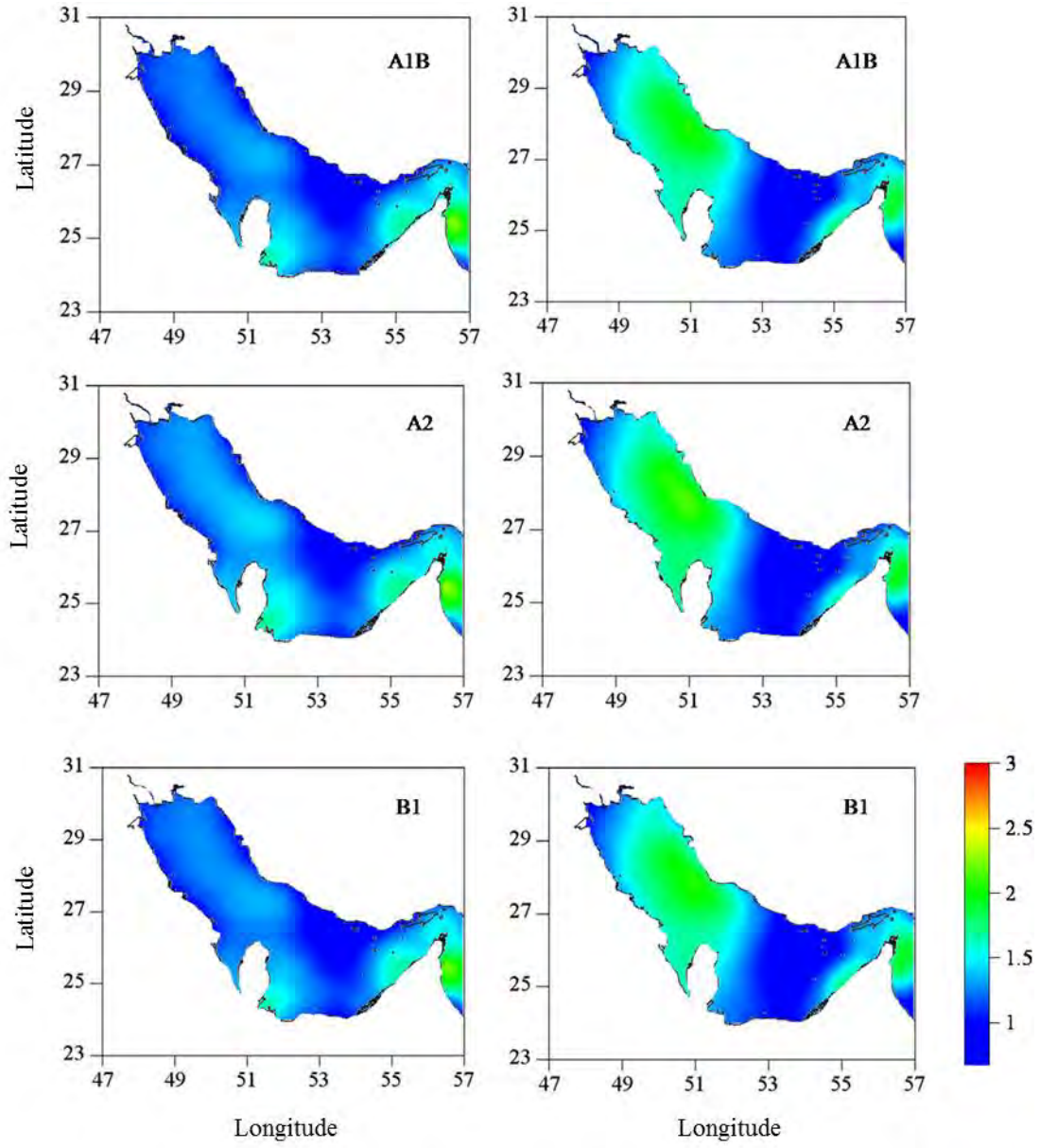

Fig. 4 β_u (left) and β_v (right) for A1B, A2 and B1 scenarios in July

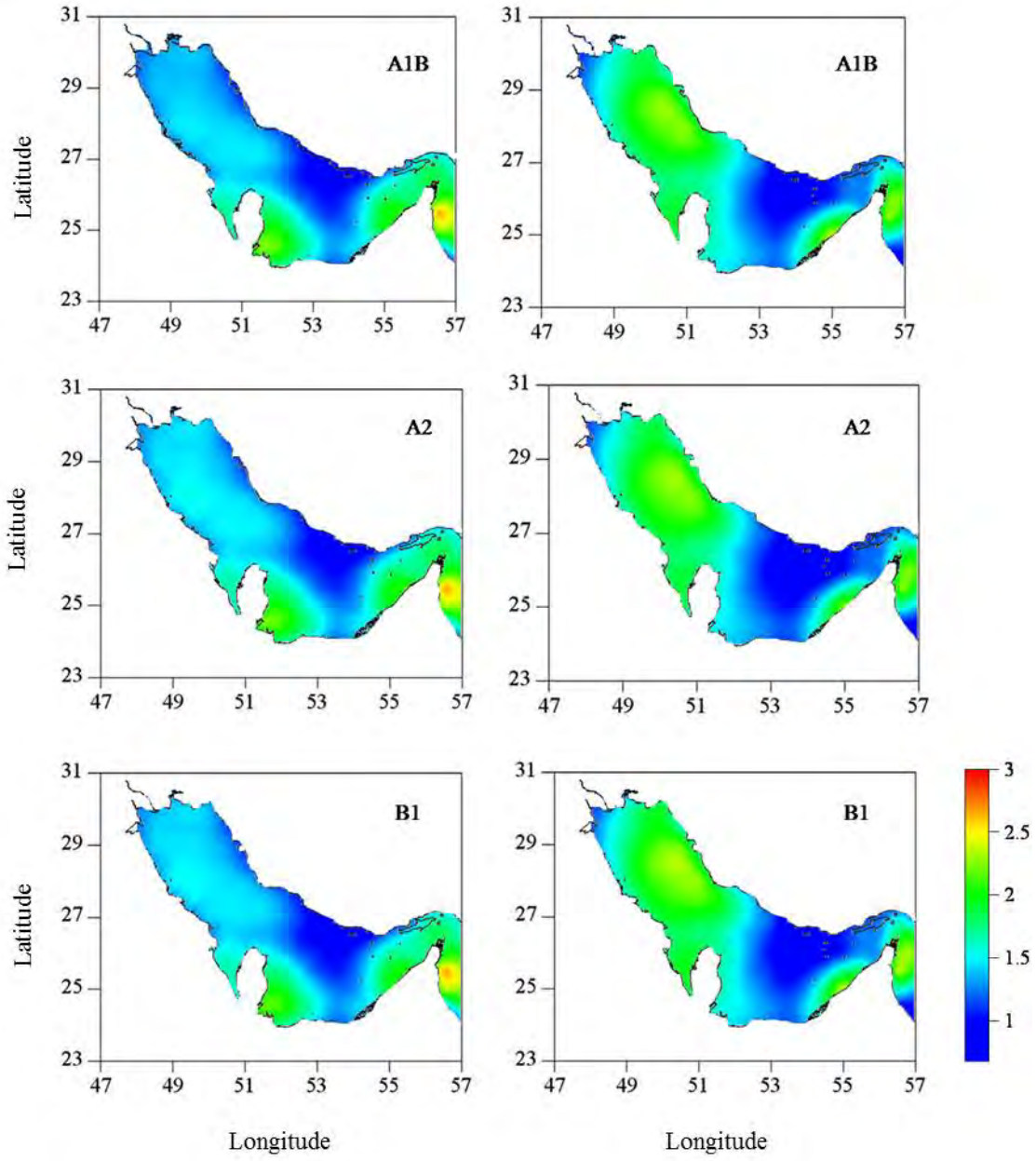

Fig. 5. β_u (left) and β_v (right) for A1B, A2 and B1 scenarios in August

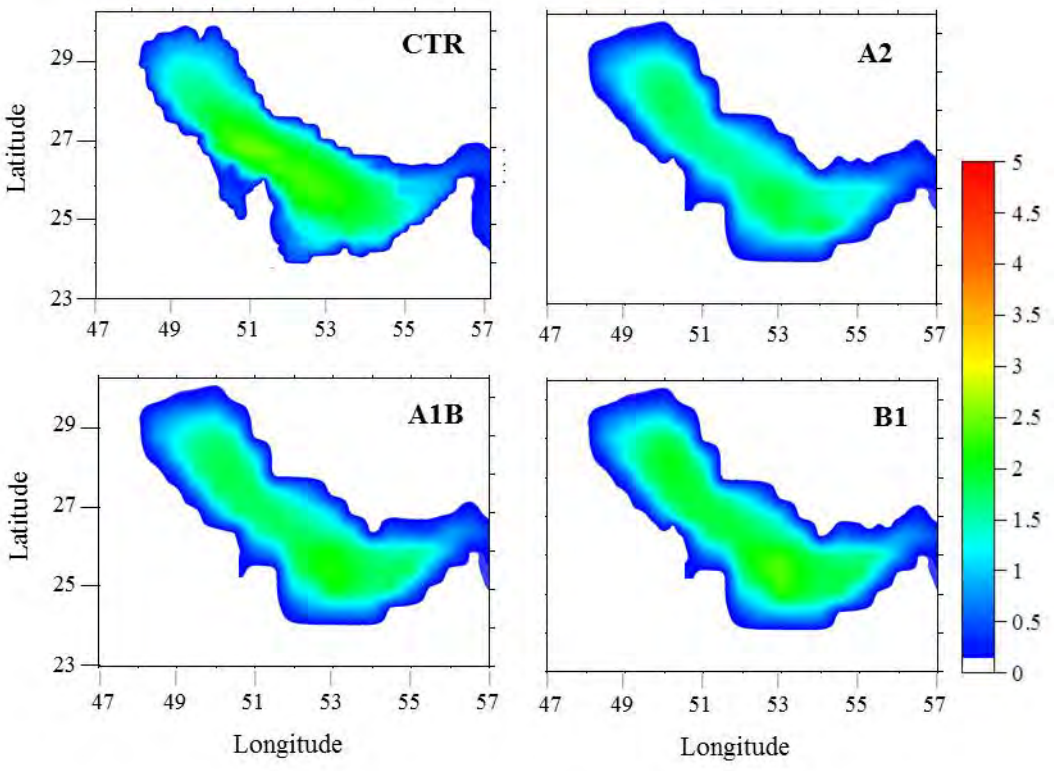

Fig. 6 Annual average of wave power (KW/m) in the Persian Gulf for control period (CTR) and scenarios

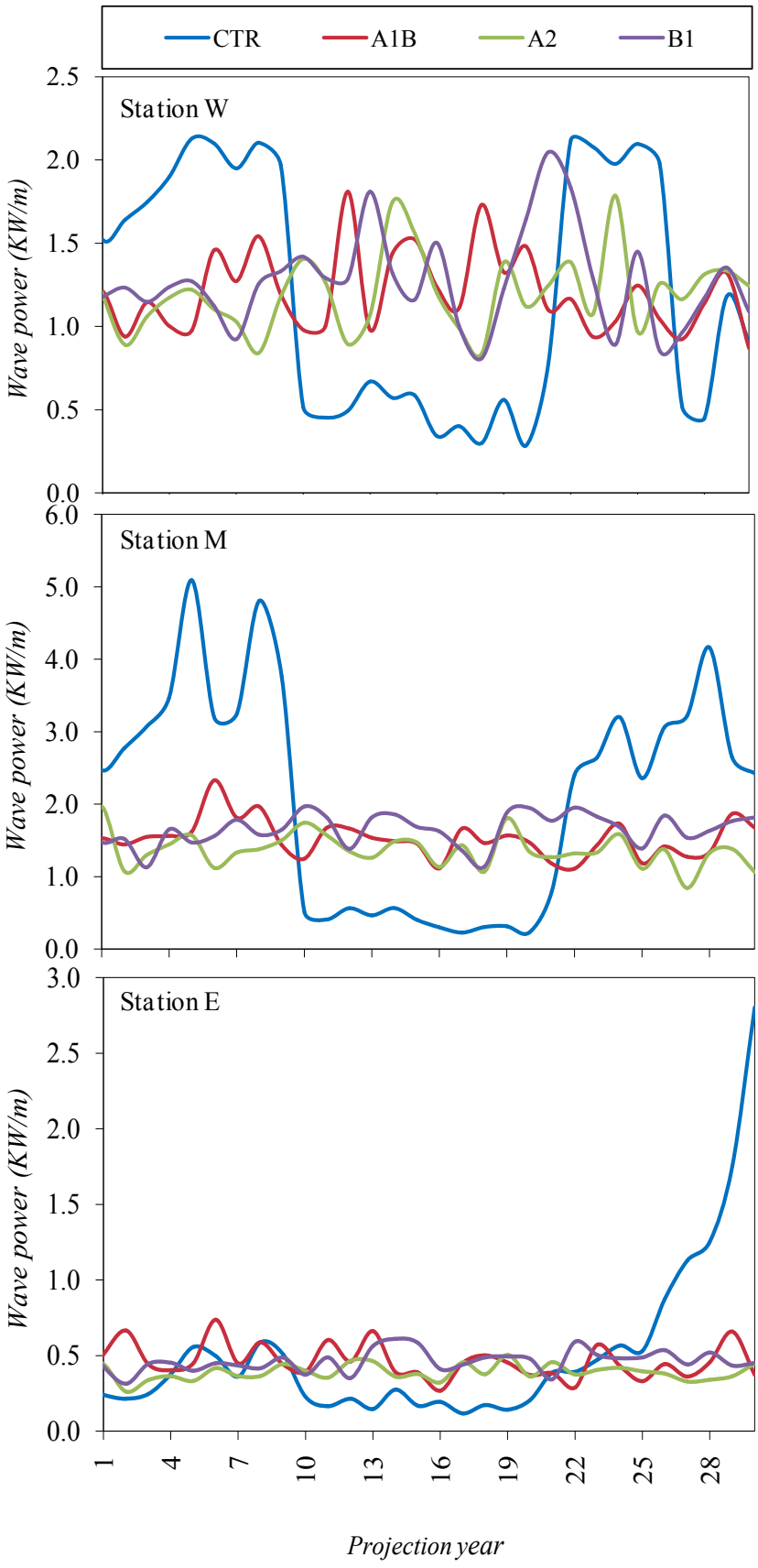

Fig. 7 Annual wave power (KW/m) in 30-yearly control and future periods in stations W, M and E

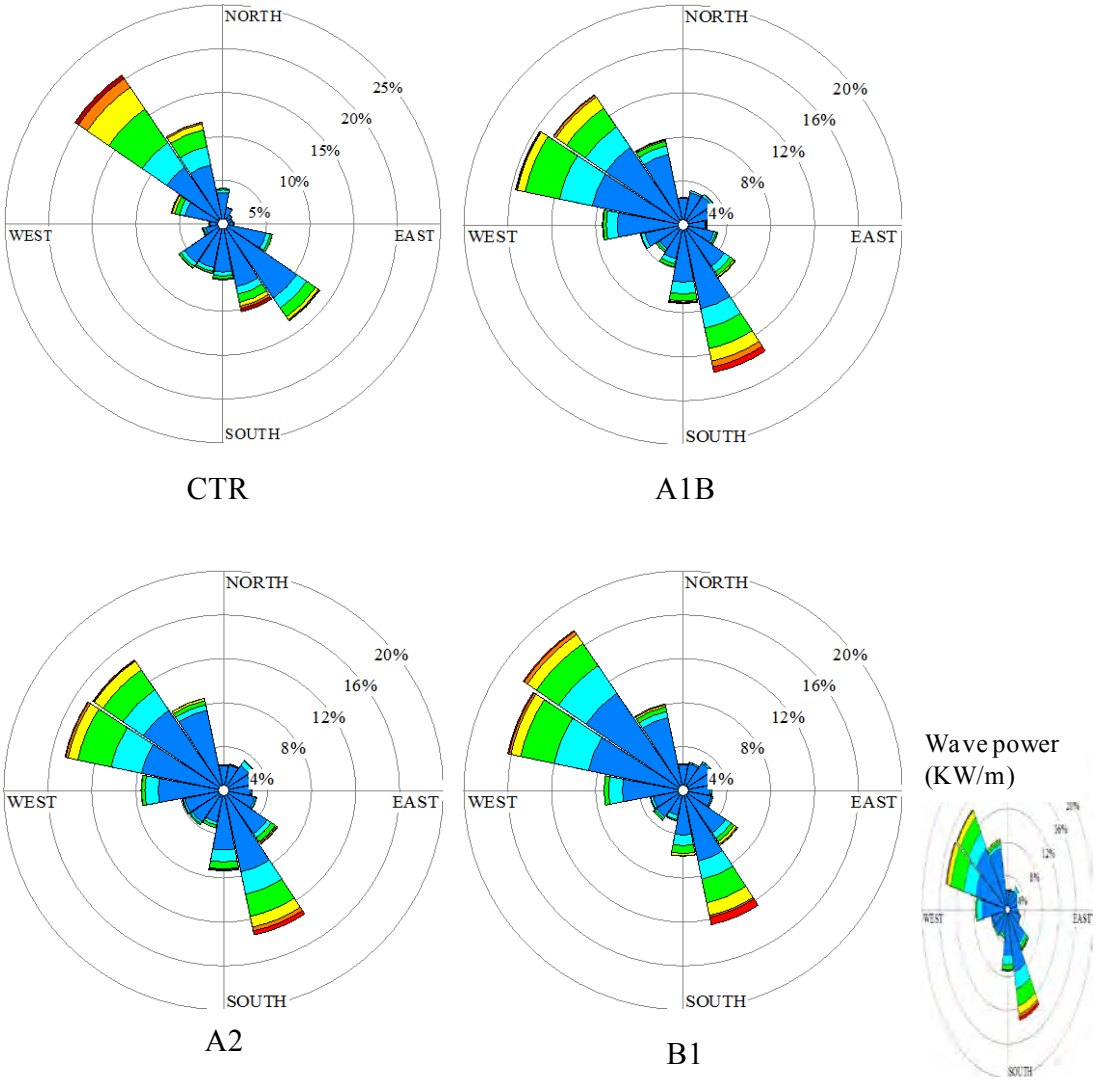

Fig. 8 Power roses in control and future periods in station W

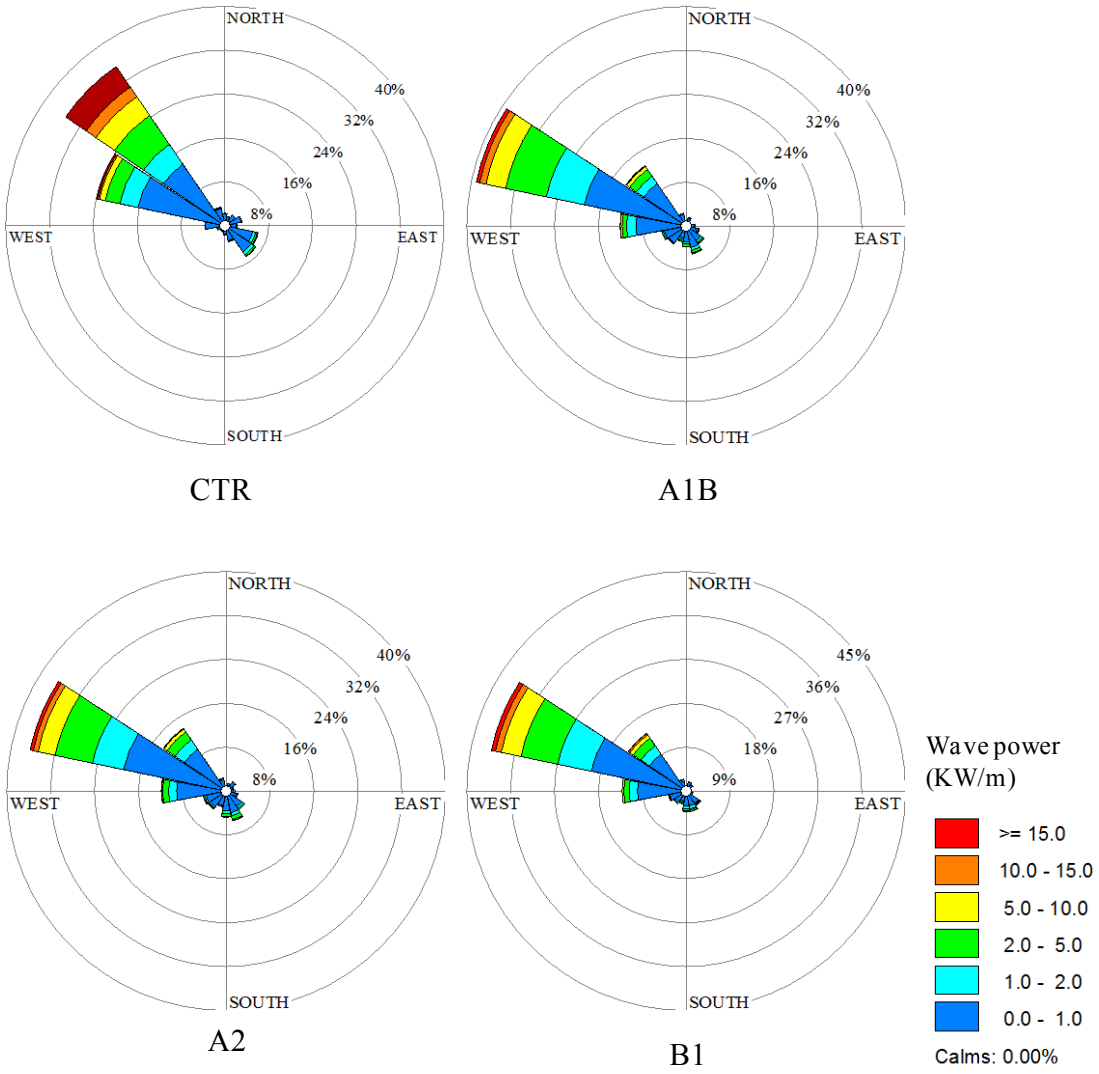

Fig. 9 Power roses in control and future periods in station M

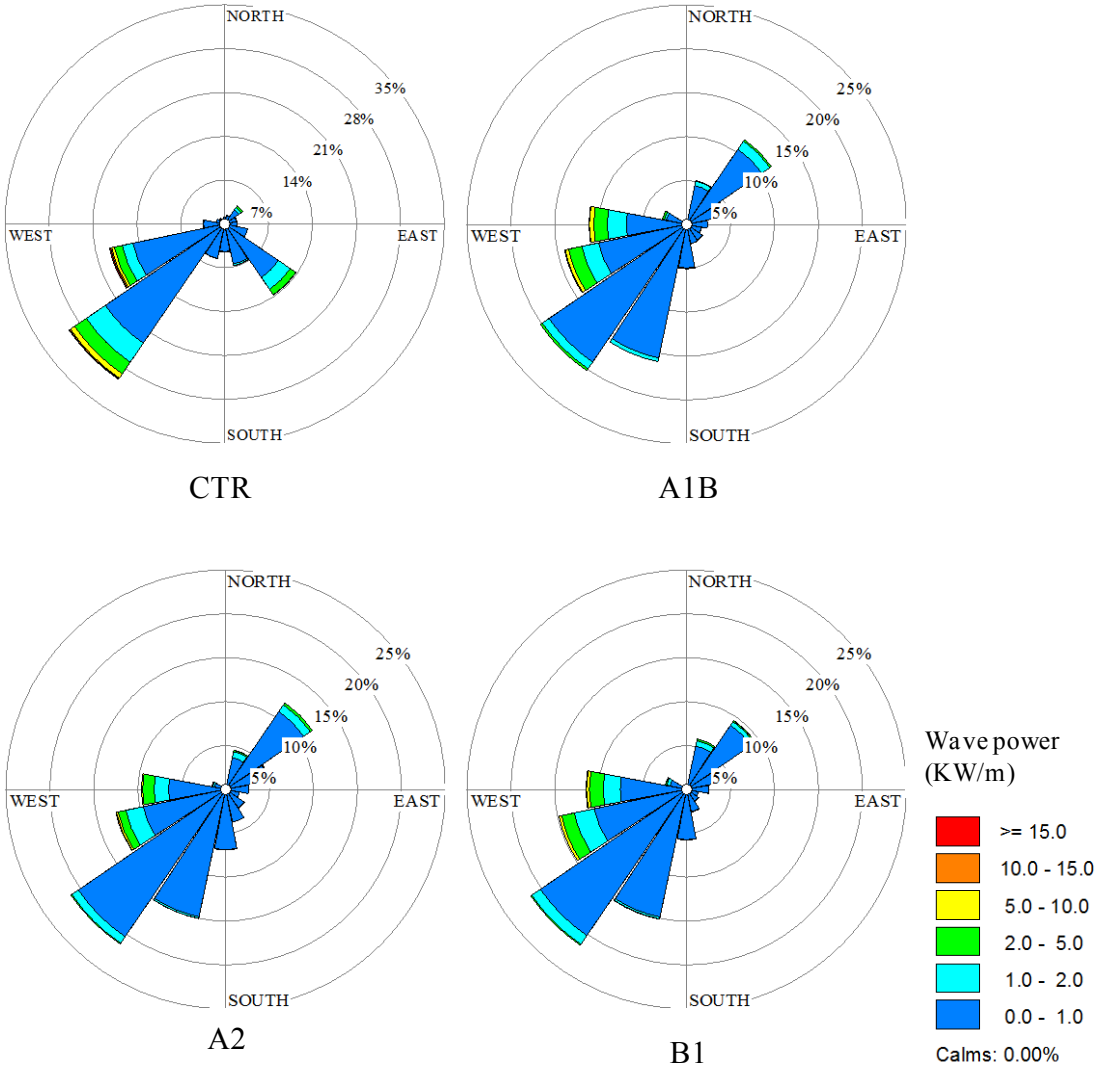

Fig. 10 Power roses in control and future periods in station E

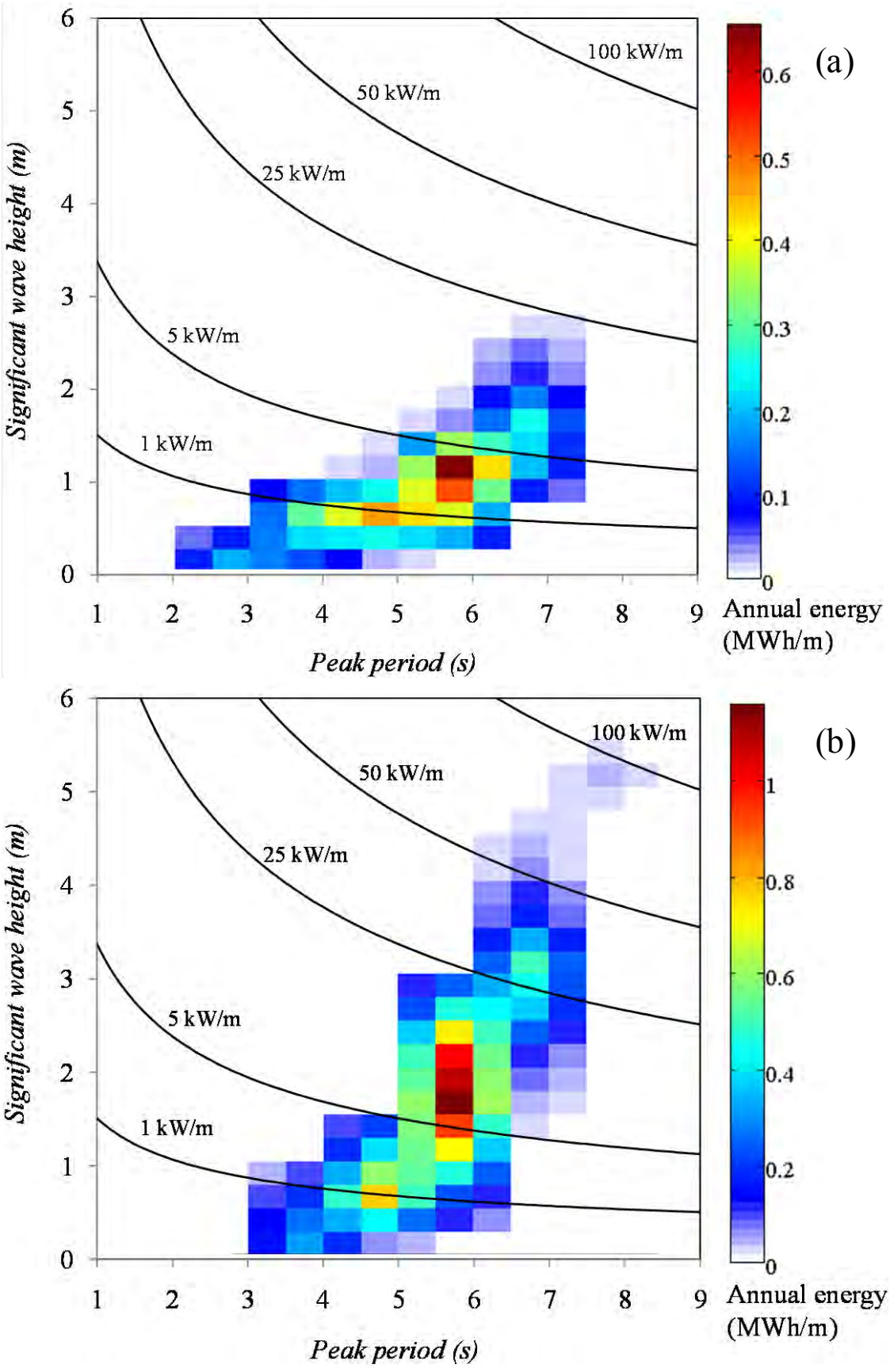

Fig. 11 Wave power distribution in control period in (a) Boushehr and (b) Assalouyeh

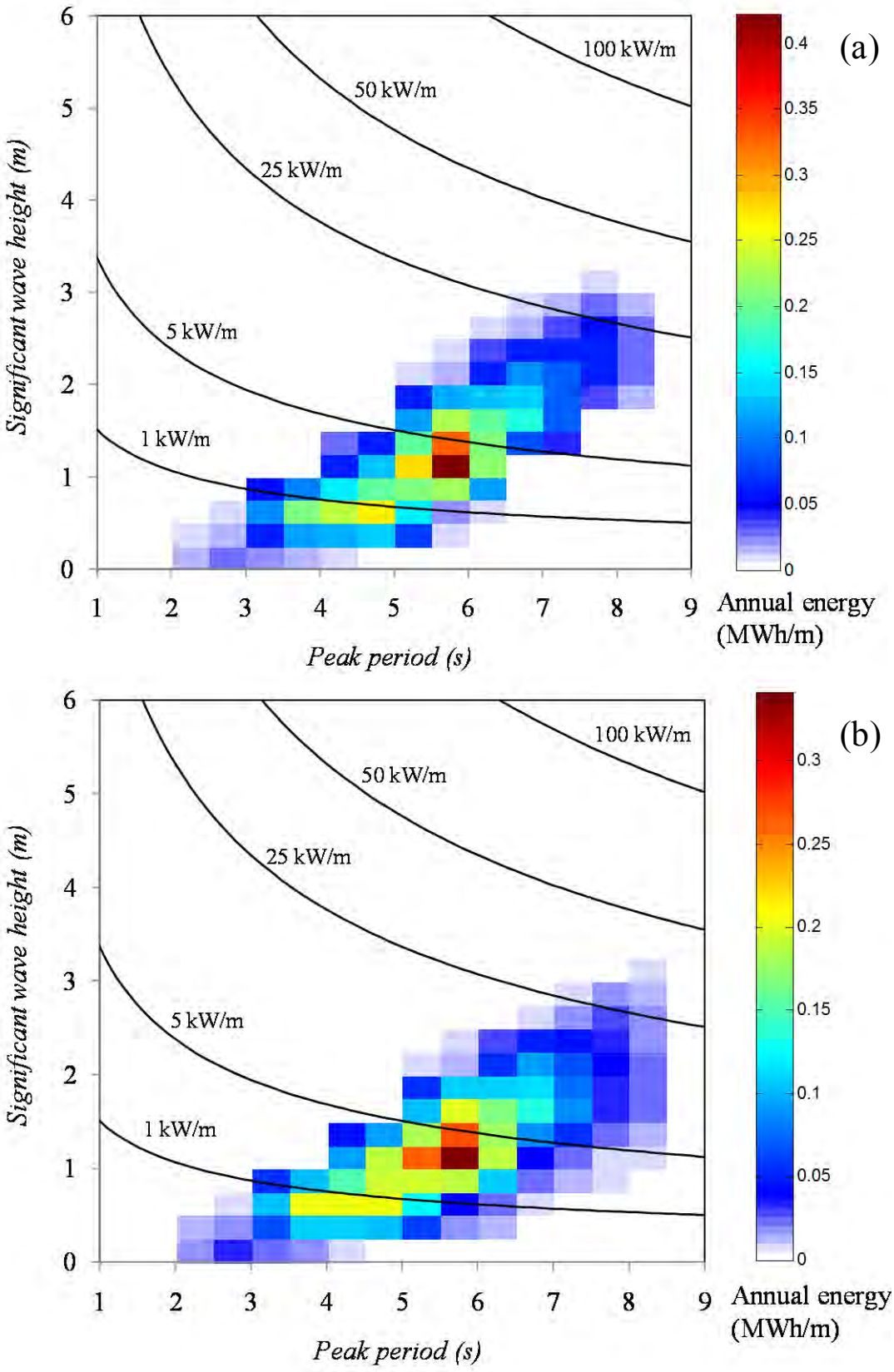

Fig. 12 Wave power distribution in (a) Boushehr and (b) Assalouyeh according to A1B scenario

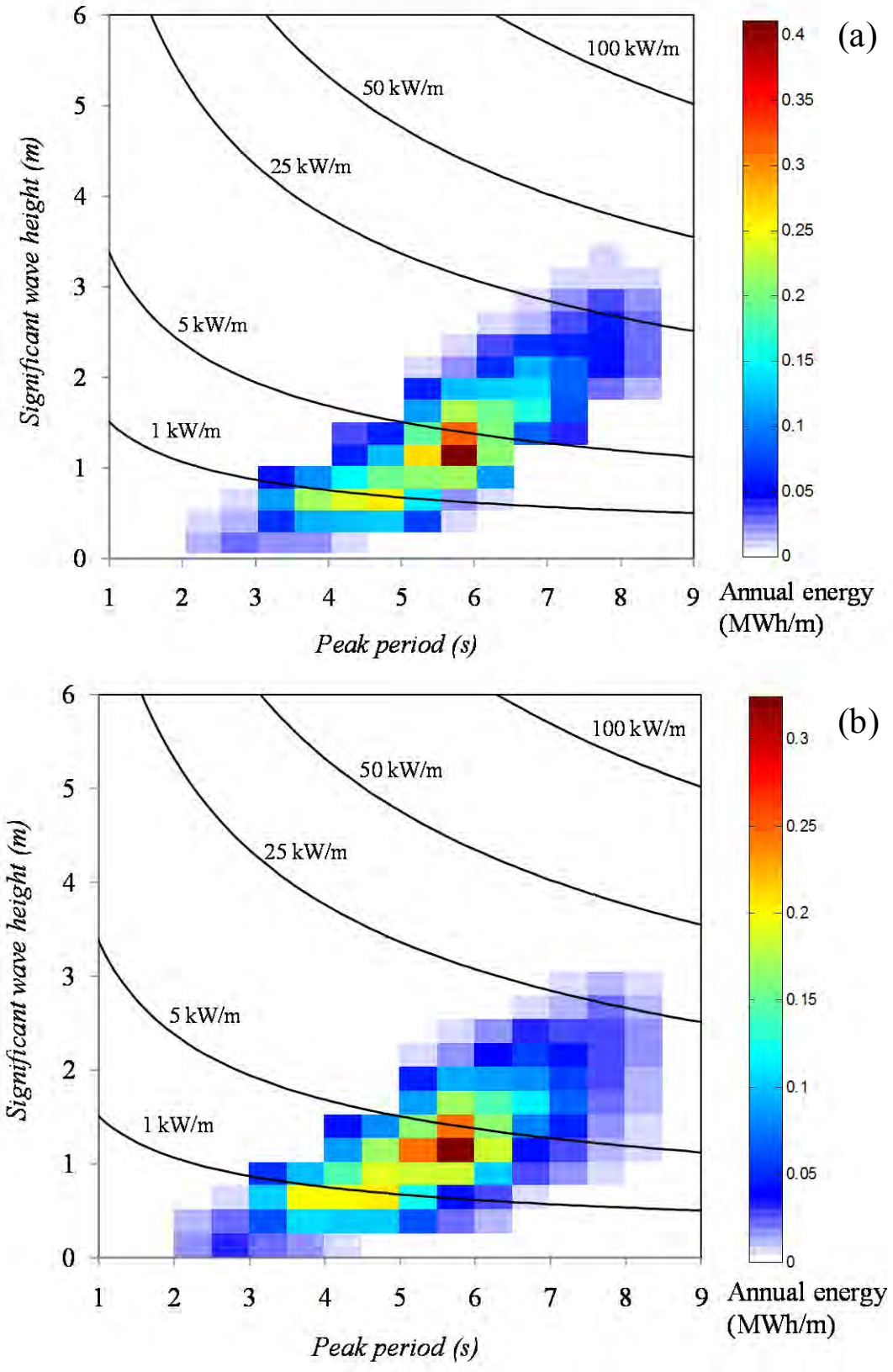

Fig. 13 Wave power distribution in (a) Boushehr and (b) Assalouyeh according to A2 scenario

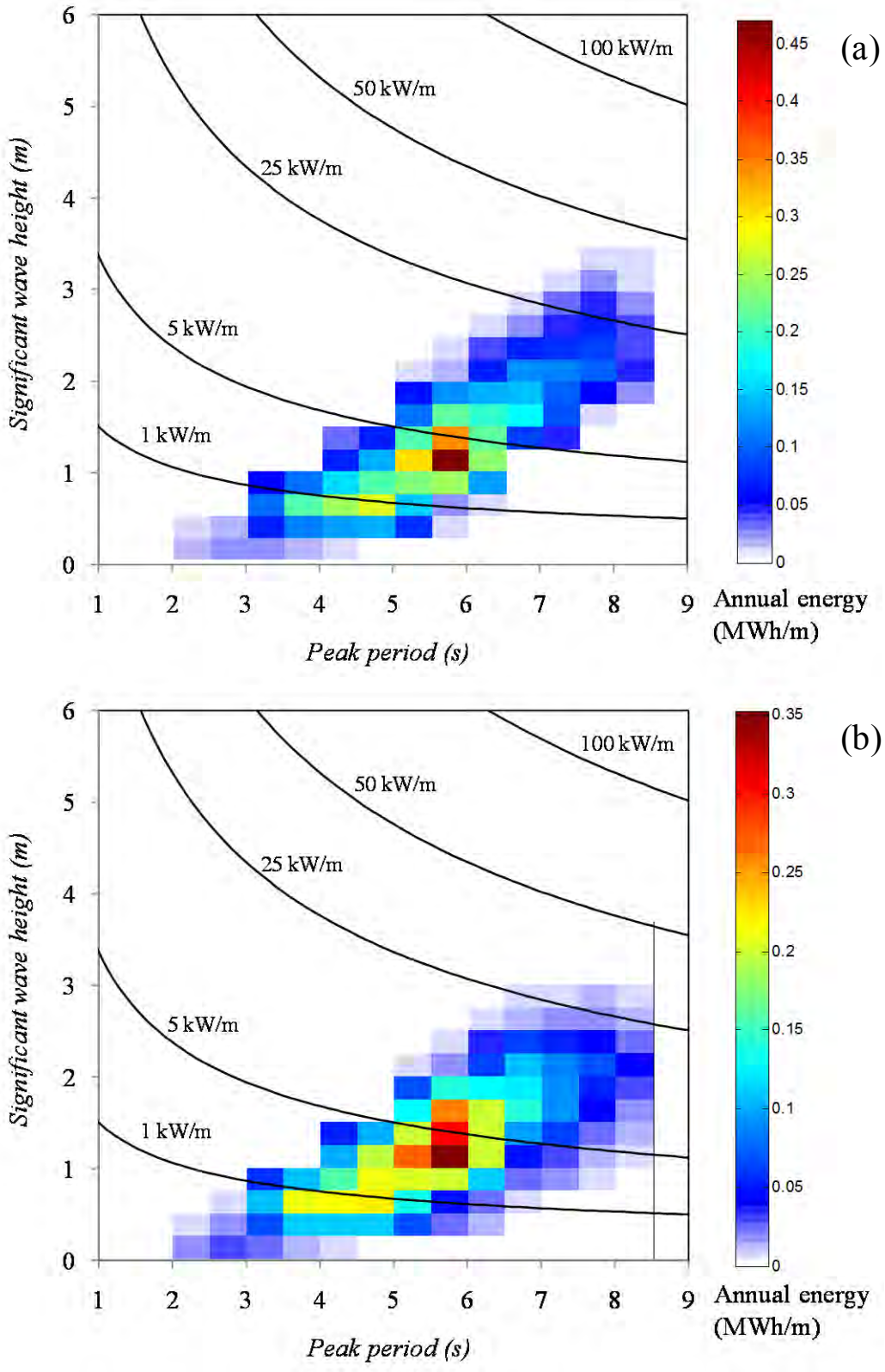

Fig. 14 Wave power distribution in (a) Boushehr and (b) Assalouyeh according to B1 scenario

Appendix

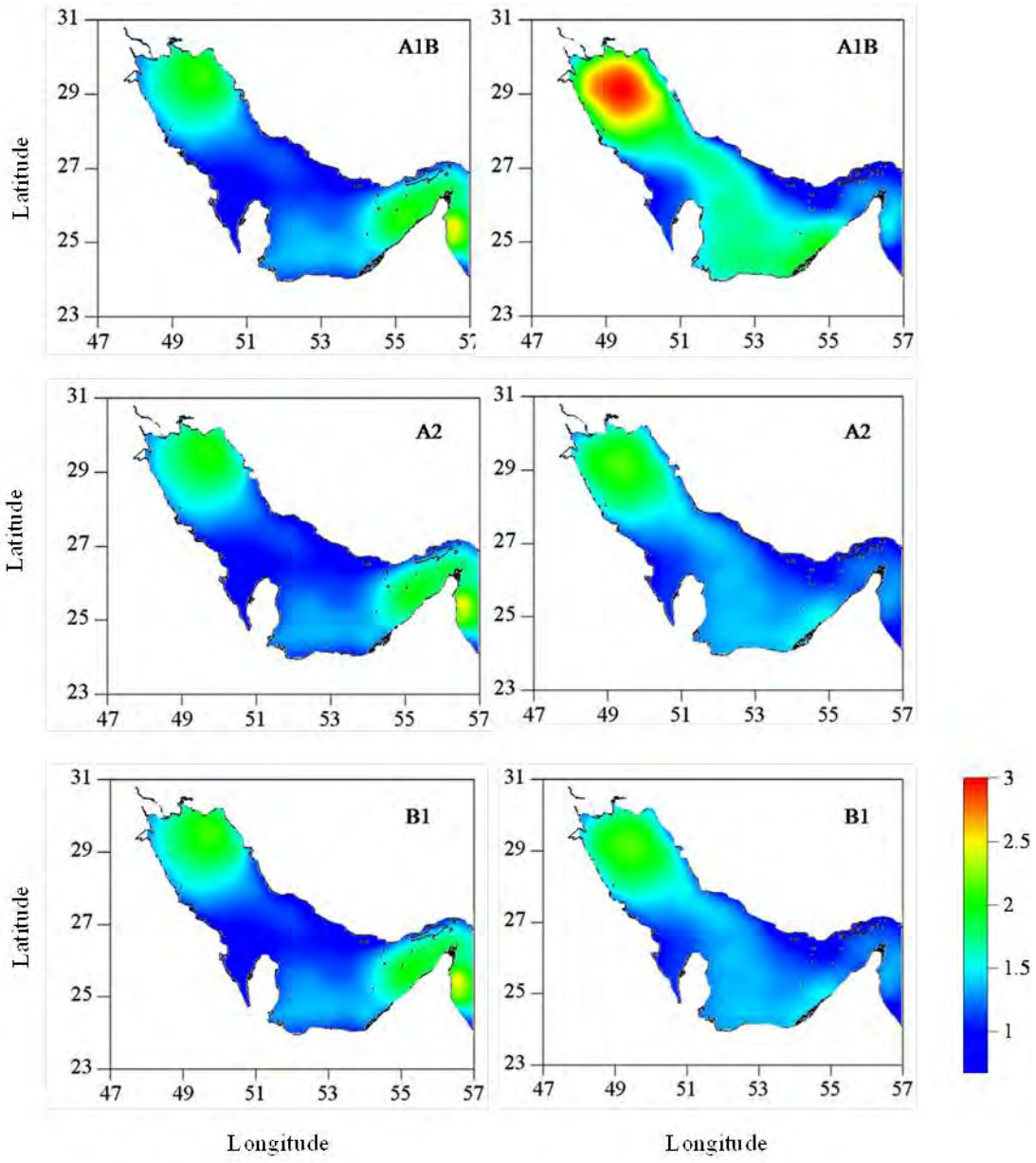

Fig. 15 β_u (left) and β_v (right) for A1B, A2 and B1 scenarios in January

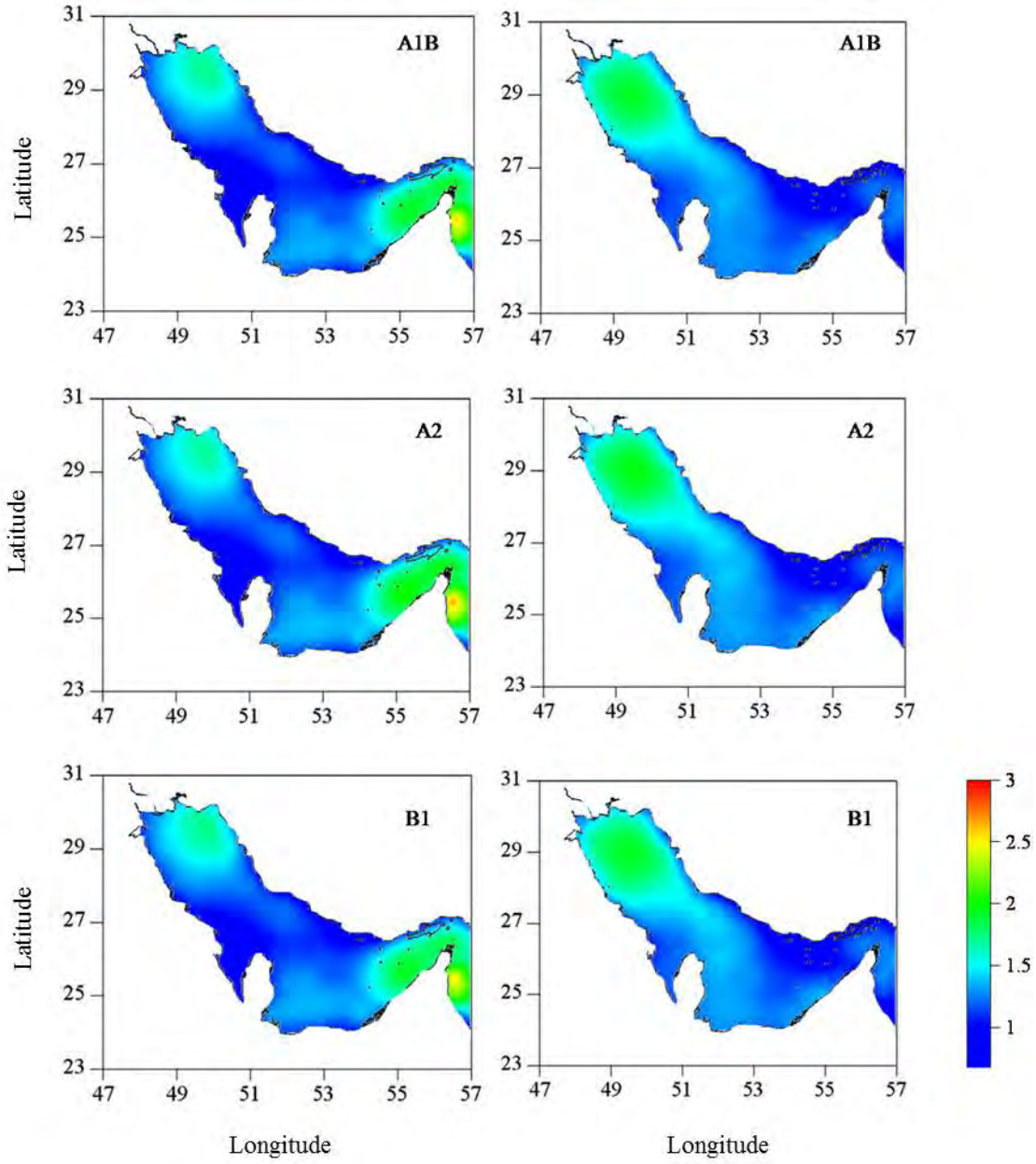

Fig. 16 β_u (left) and β_v (right) for A1B, A2 and B1 scenarios in February

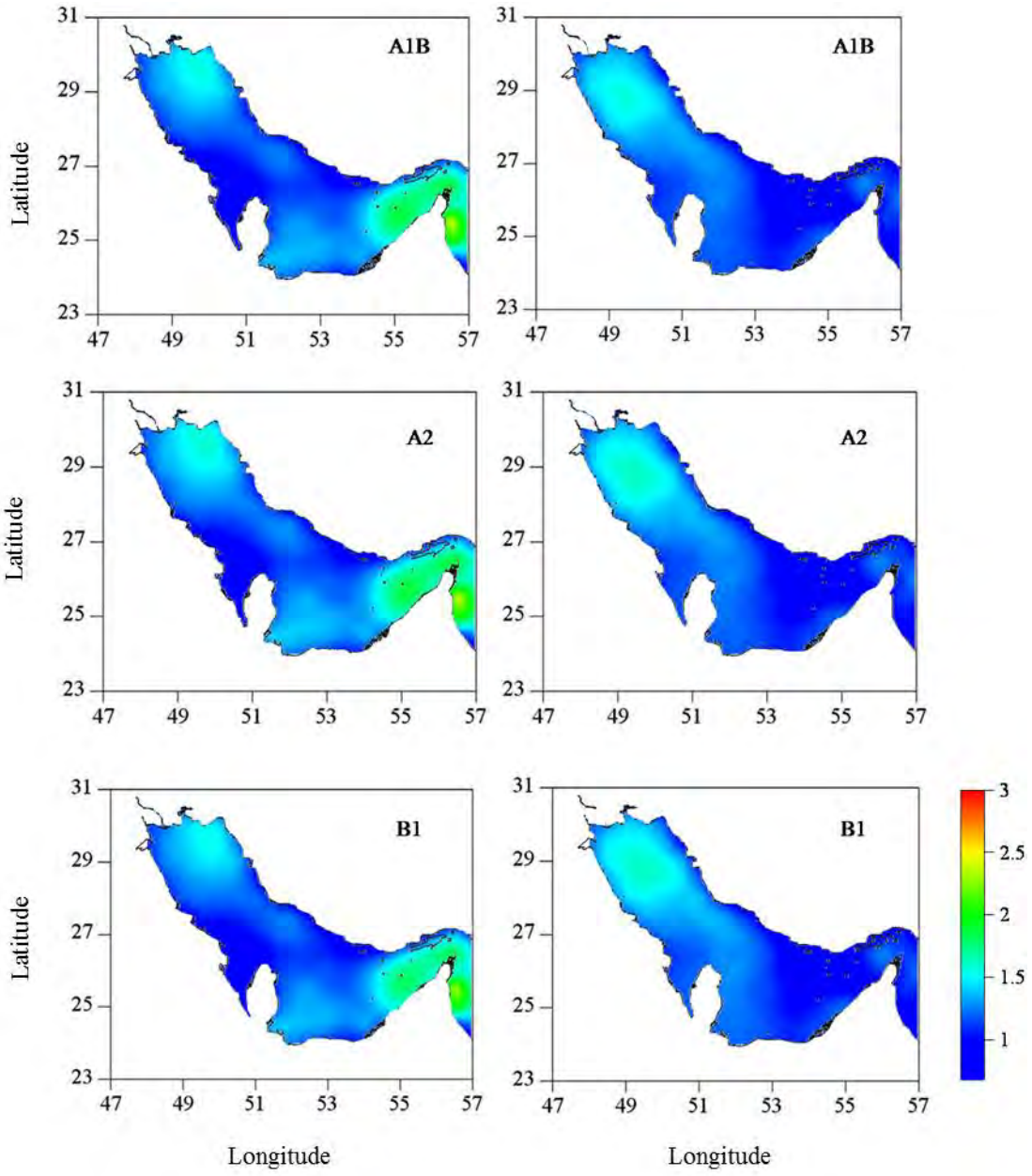

Fig. 17 β_u (left) and β_v (right) for A1B, A2 and B1 scenarios in March

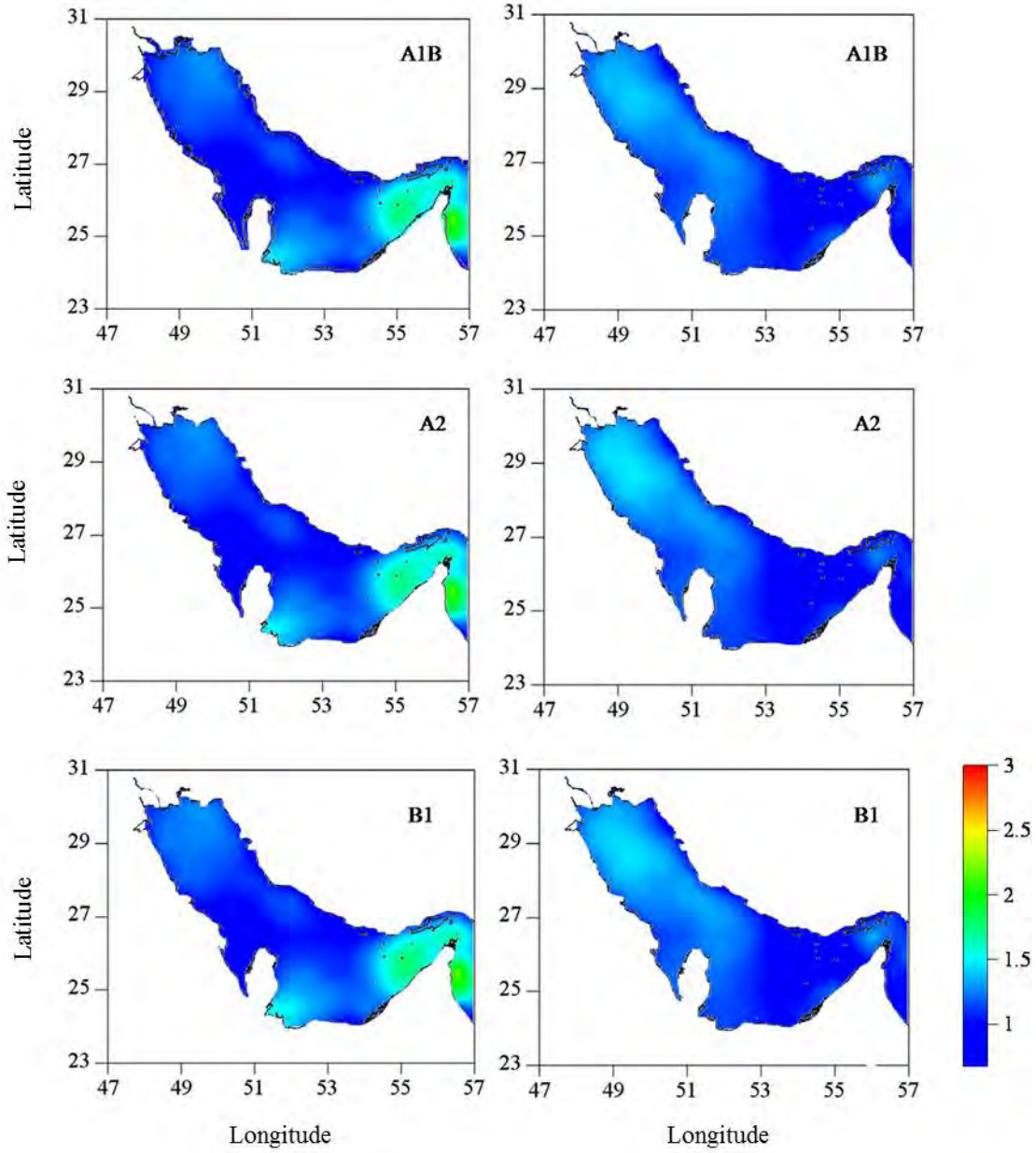

Fig. 18 β_u (left) and β_v (right) for A1B, A2 and B1 scenarios in April

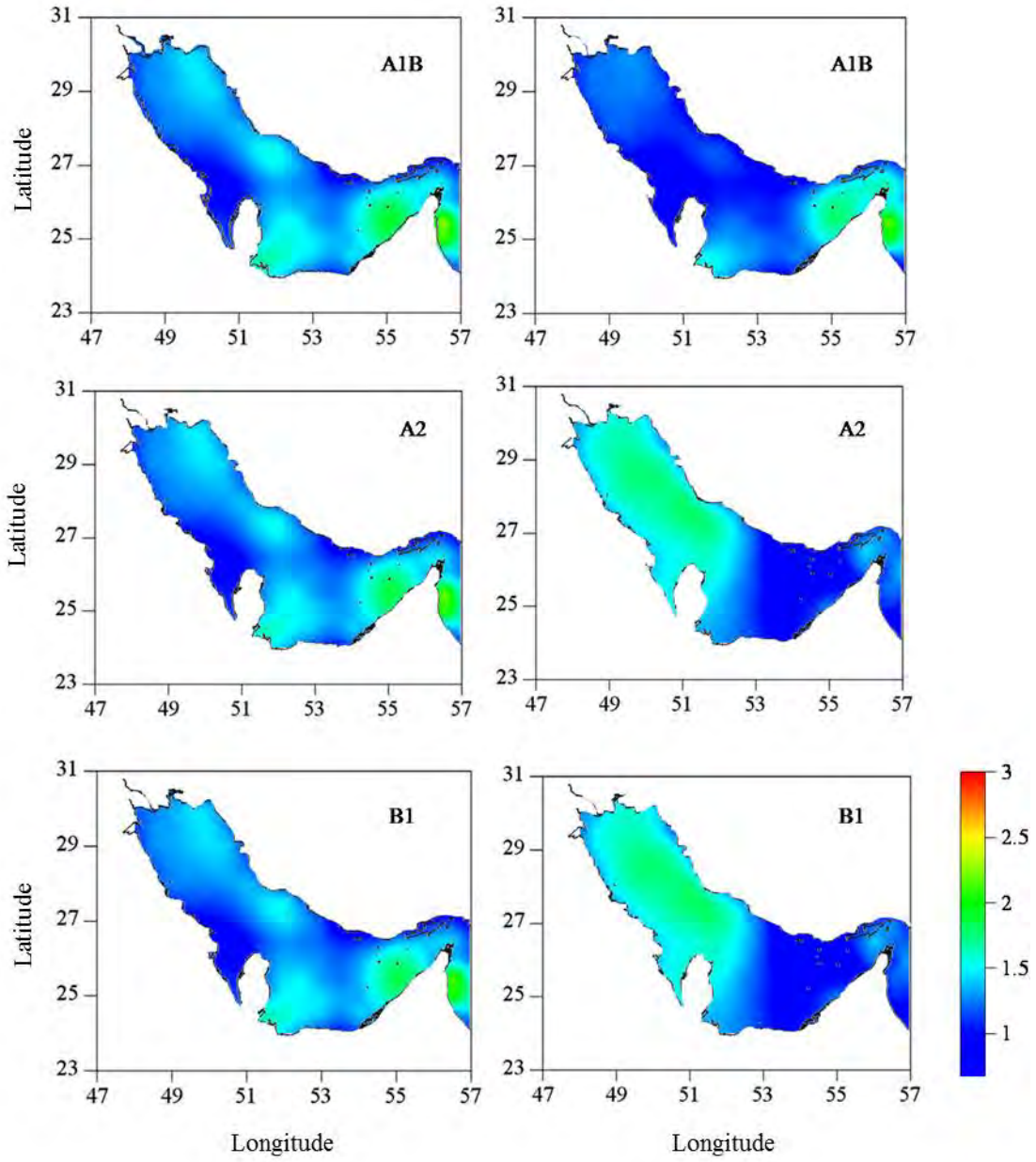

Fig. 19 β_u (left) and β_v (right) for A1B, A2 and B1 scenarios in May

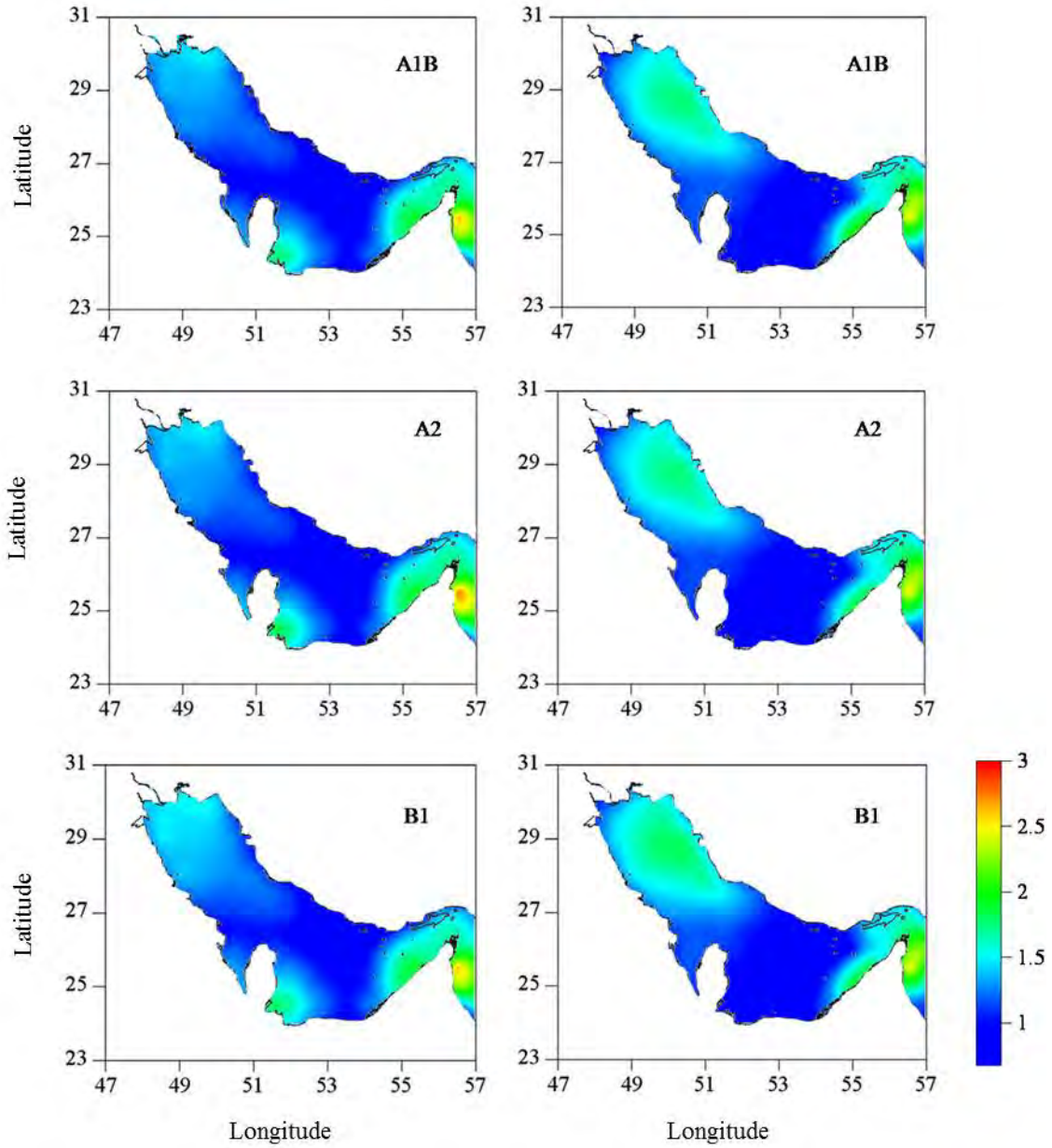

Fig. 20 β_u (left) and β_v (right) for A1B, A2 and B1 scenarios in September

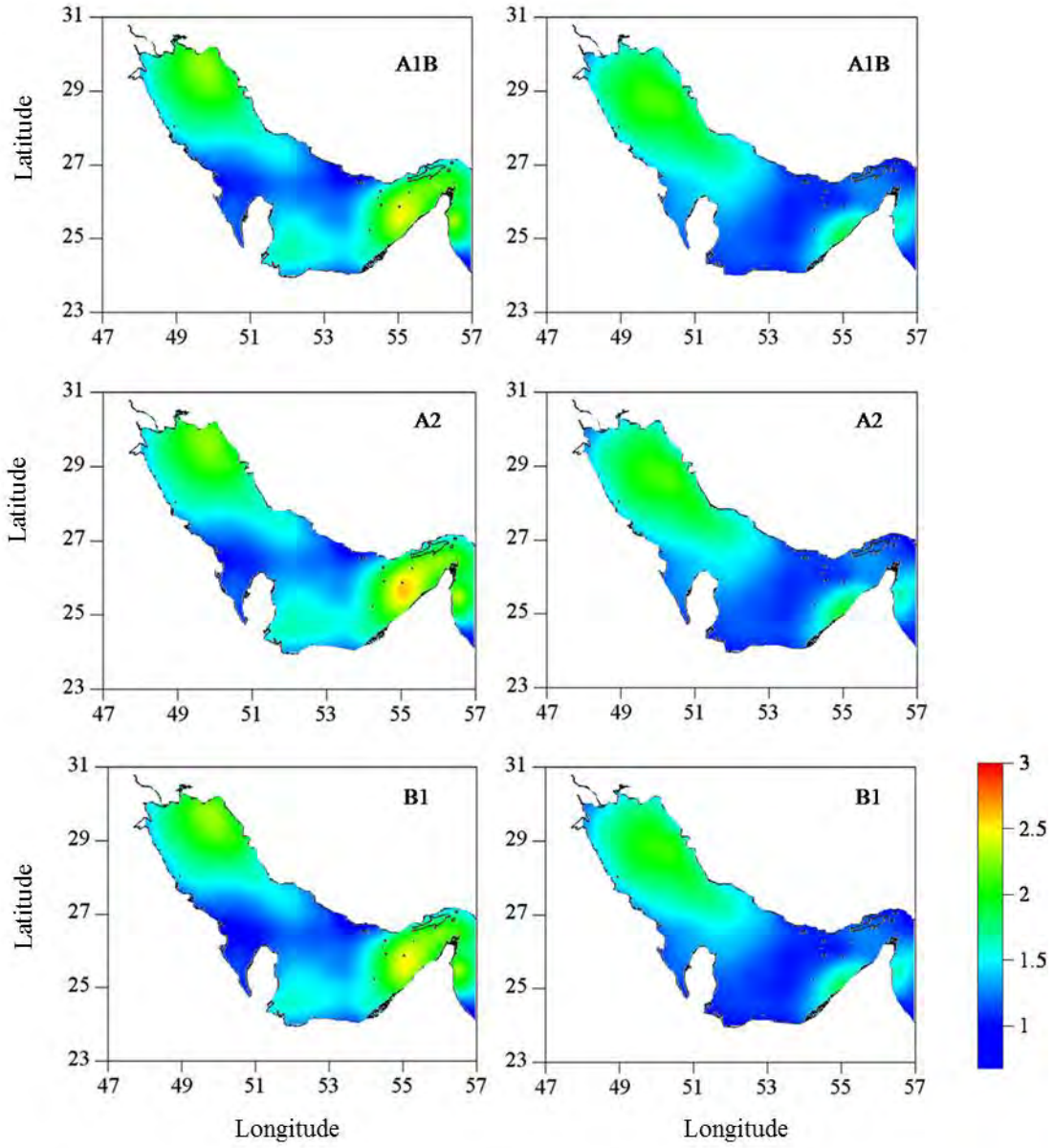

Fig. 21 β_u (left) and β_v (right) for A1B, A2 and B1 scenarios in October

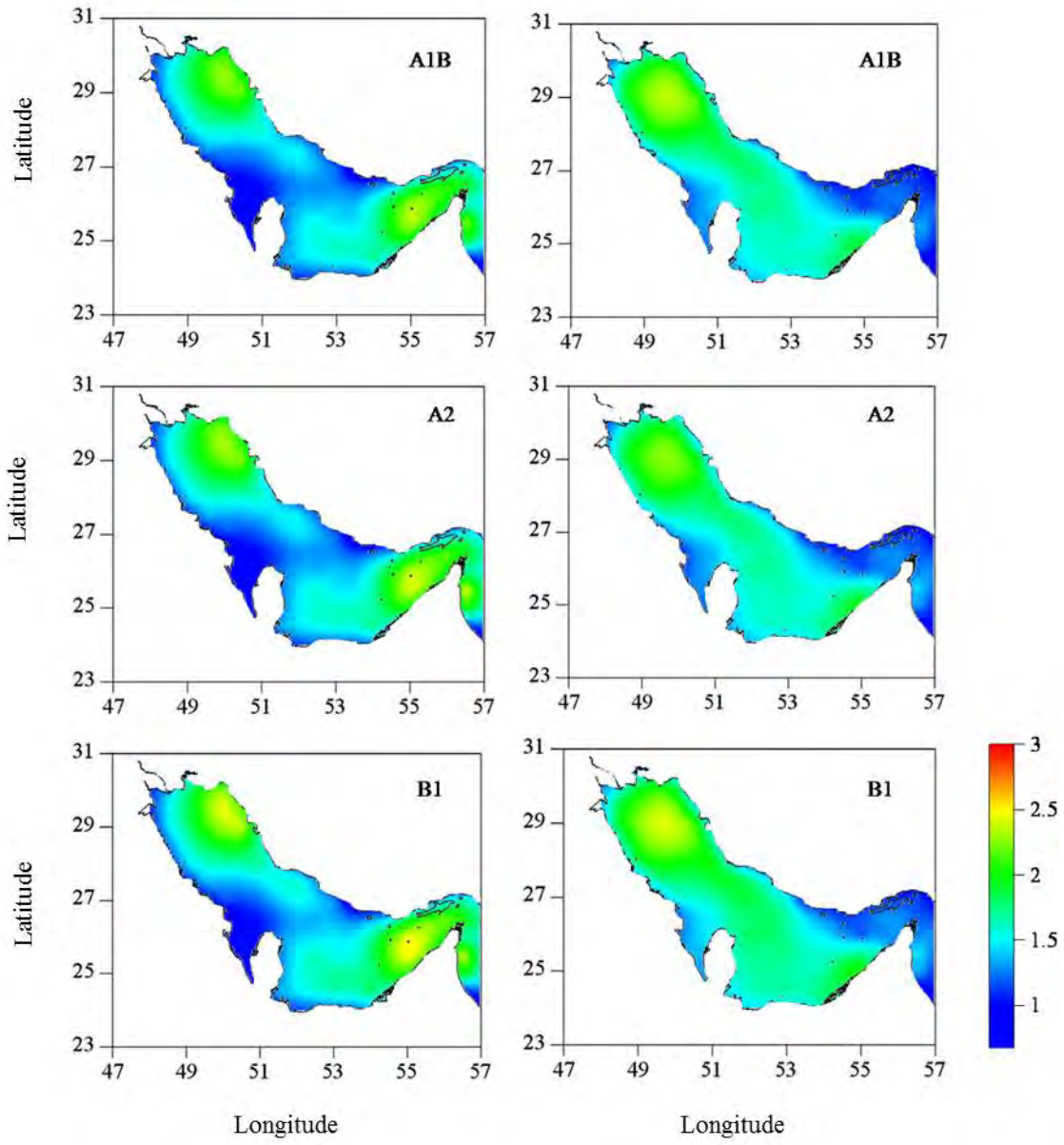

Fig. 22 β_u (left) and β_v (right) for A1B, A2 and B1 scenarios in November

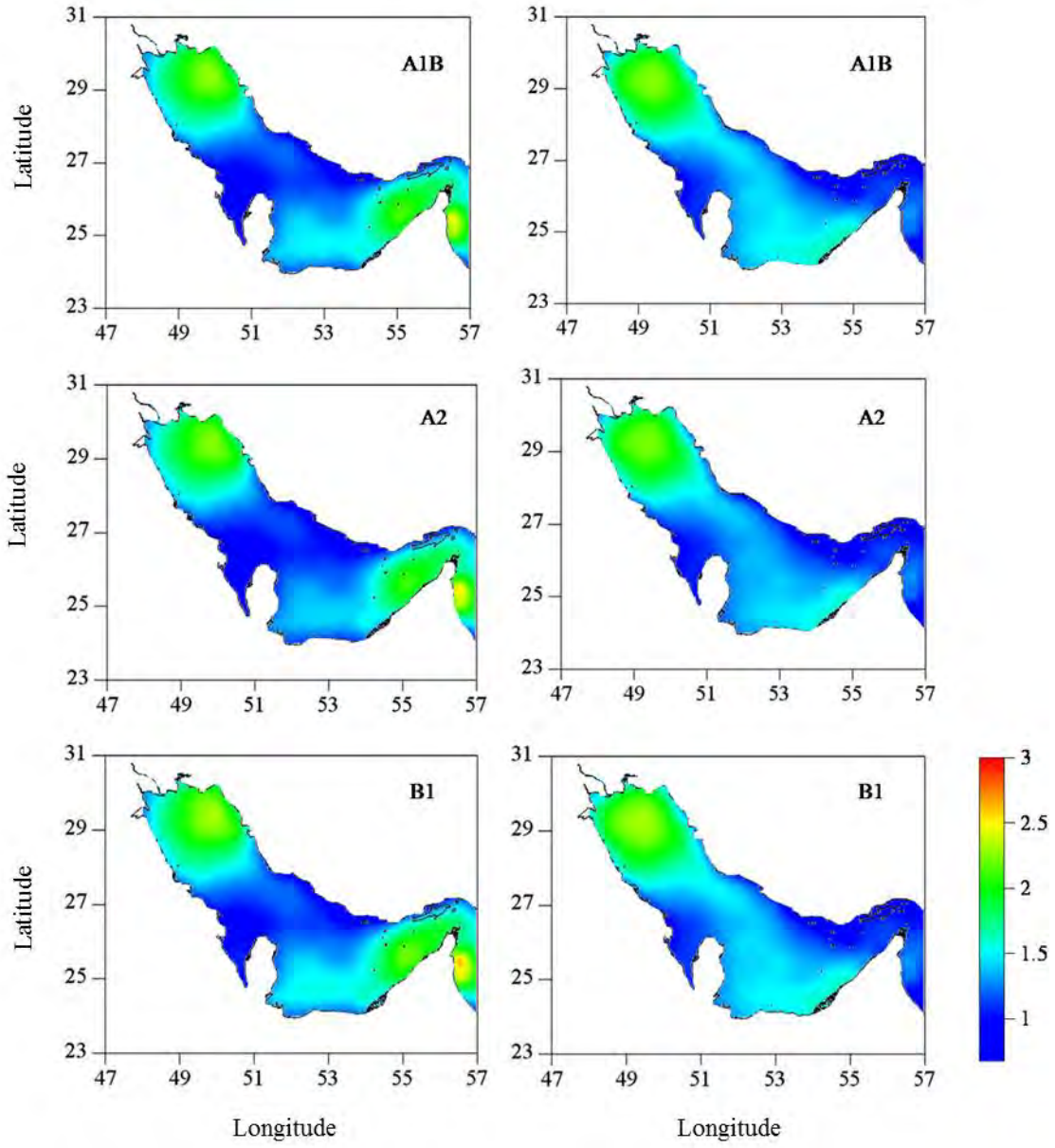

Fig. 23 β_u (left) and β_v (right) for A1B, A2 and B1 scenarios in December